

UNCLASSIFIED

AD 404 462

*Reproduced
by the*

DEFENSE DOCUMENTATION CENTER

FOR

SCIENTIFIC AND TECHNICAL INFORMATION

CAMERON STATION ALEXANDRIA, VIRGINIA



UNCLASSIFIED

NOTICE: When government or other drawings, specifications or other data are used for any purpose other than in connection with a definitely related government procurement operation, the U. S. Government thereby incurs no responsibility, nor any obligation whatsoever; and the fact that the Government may have formulated, furnished, or in any way supplied the said drawings, specifications, or other data is not to be regarded by implication or otherwise as in any manner licensing the holder or any other person or corporation, or conveying any rights or permission to manufacture, use or sell any patented invention that may in any way be related thereto.

404 462

63 3-4

**U. S. A R M Y
TRANSPORTATION RESEARCH COMMAND
FORT EUSTIS, VIRGINIA**

404462

TCREC TECHNICAL REPORT 62-100

**RECIRCULATION PRINCIPLE FOR
GROUND EFFECT MACHINES MAN-CARRYING TEST VEHICLE
PRELIMINARY FLIGHT TEST RESULTS**

Task 1D021701A04804
(Formerly Task 9R99-01-005-04)
Contract DA 44-177-TC-710

December 1962

CATALOG
AS AL

prepared by:

MARTIN COMPANY
Orlando, Florida

MAY 23 1963
TISIN A



6010

3

DISCLAIMER NOTICE

When Government drawings, specifications, or other data are used for any purpose other than in connection with a definitely related Government procurement operation, the United States Government thereby incurs no responsibility nor any obligation whatsoever; and the fact that the Government may have formulated, furnished, or in any way supplied the said drawings, specifications, or other data is not to be regarded by implication or otherwise as in any manner licensing the holder or any other person or corporation, or conveying any rights or permission, to manufacture, use, or sell any patented invention that may in any way be related thereto.

ASTIA AVAILABILITY NOTICE

Qualified requesters may obtain copies of this report from

Armed Services Technical Information Agency
Arlington Hall Station
Arlington 12, Virginia

This report has been released to the Office of Technical Services, U. S. Department of Commerce, Washington 25, D. C., for sale to the general public.

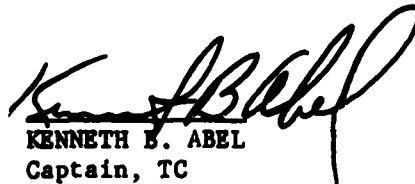
The findings and recommendations contained in this report are those of the contractor and do not necessarily reflect the views of the U. S. Army Mobility Command, the U. S. Army Materiel Command, or the Department of the Army.

HEADQUARTERS
U. S. ARMY TRANSPORTATION RESEARCH COMMAND
Fort Eustis, Virginia

This report presents the results of preliminary tests of the experimental vehicle constructed to investigate the principle of recirculation of the air cushion. This concept offers considerable theoretical promise for use in ground effect machines (GEM) in that power can be reduced for a given design operating height, both in hover and in forward flight. Additionally, the reduction in dust and spray signature is of great interest to the U. S. Army.

The results of these tests indicate that the concept is feasible and that, while design objectives were not attained, the deficiencies uncovered are not basic. The additional investigations necessary to correct deficiencies in the experimental vehicle are in progress and will be the subject of a separate report.

FOR THE COMMANDER:


KENNETH B. ABEL
Captain, TC
Adjutant

APPROVED:


WILLIAM D. HINSHAW
USATRECOM Project Engineer

(4) NH
5 552 100

(11)

Task 1D021701A04804
(Formerly Task 9R99-01-005-04)
Contract DA-44-177-TC-710
TREC Technical Report 62-100
December 1962

(6) RECIRCULATION PRINCIPLE FOR GROUND EFFECT MACHINE
MAN-CARRYING TEST VEHICLE.
PRELIMINARY FLIGHT TEST RESULTS.

7 NH
8

Final Report

10 NH (14)
OR 2830

11 - 6 -

(12) 57P

Prepared by:
Martin Company
Orlando, Florida

13 NH

14 44 177-2

for

U. S. ARMY TRANSPORTATION RESEARCH COMMAND
FORT EUSTIS, VIRGINIA

(16)

NH

(17) ATREC

(19) TR 2 / 100

11

12

FOREWORD

This report presents the results of an experimental investigation of the hovering performance and of the stability and control characteristics of a recirculation ground effect machine (GEM). The work was sponsored by the U. S. Army Transportation Research Command under Contract DA-44-177-TC-710 and was conducted through the period from March 1962 to June 1962.

Mr. P. Vinson was the principal investigator on this study and was assisted by Messrs. J. Butsko, G. Martin, C. E. Middlebrooks, and A. Ortell. This report has been reviewed and approved by K. R. Cossairt, GEM Project Engineer.

ILLUSTRATIONS

<u>Figure</u>		<u>Page</u>
1	Preloaded on Overhead Support System	5
2	Initial Run-up of Engines	6
3	Tethered Hovering Tests	7
4	Evaluating Control Effectiveness	8
5	Base Instrumentation	9
6	AiResearch Bleed Engine Performance	11
7	Effect of Water Injection on Bleed Flow	12
8	Effect of Water Injection on Bleed Temperature and Pressure	13
9	Schematic, Ejector Components	15
10	Comparison of 2-D and 3-D Base Pressures	16
11	Comparison of 2-D and 3-D Base Pressures	18
12	Effect of Increased Primary Mass Flow on Base Pressure	19
13	Effect of Inner Flap Setting on Base Pressure	20
14	Effect of Inner Flap Setting on Base Pressure	21
15	Effect of Outer Flap Setting on Base Pressure	22
16	Effect of Outer Flap Setting on Base Pressure	23
17	Effect of Ejector Flap Angles on Base Pressure	24
18	Recirculating Ejector Flow at Design Height	26
19	Recirculating Ejector Flow at Lower Than Design Height	27
20	Recirculating Ejector Flow at Greater Than Design Height	28
21	Effect of Uniform Ejector Tilt-on Base Pressure	29
22	Cavity Pressure Variation with Height	31
23	Effect of Water Injection on Base Pressure	32
24	Effect of Surface Irregularity on Base Pressure	33
25	Effect of Surface Roughness for 2-D Tests	34

<u>Figure</u>		<u>Page</u>
26	Effect of Surface Roughness for 2-D Tests	35
27	Comparison of Theory and Experiment for Base Pressure and Cavity Pressure	37
28	Comparison of Theory and Experiment for Base Pressure and Cavity Pressure	38
29	Comparison of Theory and Experiment for Base Pressure and Cavity Pressure	39
30	Lift versus Height	40
31	Schematic, Pitch Stability	44
32	Theoretical and Experimental Curve for Mass Augmentation and Minimum Height for Positive Stability in Pitch, Wind Tunnel Model	45
33	Minimum Height for Positive Stability of the Small Scale wind Tunnel Model in Pitch	46
34	Minimum Height for Cavity Pressure Stability	48
35	Effect of Base Tilt on Base Pressure with Controls Locked in Neutral Position	49
36	Control Effectiveness Test	51
37	Effect of Ejector Area Ratio and Primary Pressure on Base Pressure	54

LIST OF SYMBOLS

a	Vehicle Characteristic Width	ft
b	Vehicle Characteristic Length	ft
C	Circumference	ft
g	Acceleration Due to Gravity	32.17 ft/sec ²
h	Height of Base Above Ground	in
j	Momentum Flux of Ejector Exit Flow per Unit Length	lb/ft
j'	Momentum Flux of Primary Flow per Unit Length	lb/ft
\int	Lift	lb
L	Rolling Moment	ft/lb
M	Pitching Moment	ft/lb
m	Total Mass Flow at Ejector Exit	lb/sec
m'	Total Primary Mass Flow	lb/sec
P _a	Ambient Pressure (Gage)	psfg
P _{o'}	Total Pressure in Primary Nozzles (Gage)	psig
P _{Tj}	Average Total Pressure of Recirculating Flow (Gage)	psfg
P _B	Average Base Pressure (Gage)	psfg
P _C	Cavity Pressure (Gage)	psfg
T _a	Ambient Temperature	Degrees Fahrenheit
t	Ejector Mixing Section Thickness	in
t _e	Ejector Exit Thickness	in
V _j	Average Recirculating Flow Velocity	ft/sec
α	Pitch Angle from Horizontal	Degrees
β	Ejector Tilt Angle from Horizontal	Degrees
θ_1	Ejector Inlet Angle from Horizontal	Degrees
δ_{\bullet}	Outer Ejector Exit Flap Angle from Horizontal	Degrees
δ_i	Inner Ejector Exit Flap Angle from Horizontal	Degrees
ϵ	Ejector Efficiency	
ρ	Density of Air	lb/ft ³
θ_2	Ejector Exit Angle from Horizontal	Degrees

SUMMARY

This final report presents the results of a preliminary experimental evaluation of a recirculation ground effect machine conducted by the Martin Company. The GEM vehicle tested was of rectangular planform type with base dimensions of 12 feet by 15 feet. Lift power was supplied by two AiResearch GTC 85 series bleed air jet engines. Since the vehicle was intended primarily as a hovering test bed, forward propulsion was not specifically provided.

The vehicle was evaluated with respect to lift capability, static stability, and control effectiveness. Dust and spray characteristics were observed over land and water respectively.

CONCLUSIONS

The feasibility of obtaining lift by utilizing the recirculating ejector concept was proven. Although various sources of losses prevented attainment of 2-D base pressure level, sufficient lift was developed to support the vehicle at less than design height.

The vehicle was observed to be neutrally stable or slightly unstable in pitch and roll at the heights attained. This lack of positive static stability at low heights was observed in the small scale wind tunnel model and correlates well with the analytical studies presented herein. With the present configuration, the vehicle would be stable at heights over 16 inches. Unfortunately, this height was unattainable with the available lift power plants. The lack of pitch and roll stability precluded obtaining forward flight data.

RECOMMENDATIONS

The two-dimensional experimental data indicates that a lift power plant, capable of delivering 12 to 15 lb/sec of airflow at 8 to 10 psig, would improve the ejector efficiency by 50 percent and provide sufficient base pressure to hover at an 18-inch height, utilizing a 375 to 400 horsepower lift engine. The vehicle is predicted to be stable and controllable in this condition.

It is therefore recommended that the following steps be taken to modify the vehicle:

1. Conduct additional 2-D ejector tests at area ratios of 10 to 100 to verify ejector performance characteristics.
2. Redesign corner ejectors to eliminate corner leakage and minimize or eliminate 2-D versus 3-D performance loss.
3. Obtain and install a lift power plant compatible with ejector requirements from step 1 above.

DISCUSSION OF RESULTS

INTRODUCTION

The development of the recirculating ejector theory for base pressurization and subsequent verification of this theory in two-dimensional and in small scale three-dimensional experimental programs reported in References 1 and 2 was followed by the construction and evaluation of a full-scale man-carrying test vehicle (MCTV). Construction of the test vehicle is reported in Reference 3. This report presents the experimental results of a preliminary evaluation program conducted on this vehicle.

The vehicle was designed primarily as a hovering test bed to demonstrate the feasibility of utilizing ejector recirculation for the lifting system. Forward propulsion was therefore not specifically provided, although it was anticipated that the residual thrust of the lift engines would provide forward speeds of up to 20 mph.

The test program was designed to investigate hovering performance, static stability, control effectiveness, and low speed forward flight effects. The instrumentation was limited to water manometers, pressure gages, visual observations, and photographic coverage. Figures 1 through 4 show typical scenes from the test program. Base pressure instrumentation is shown in Figure 5.

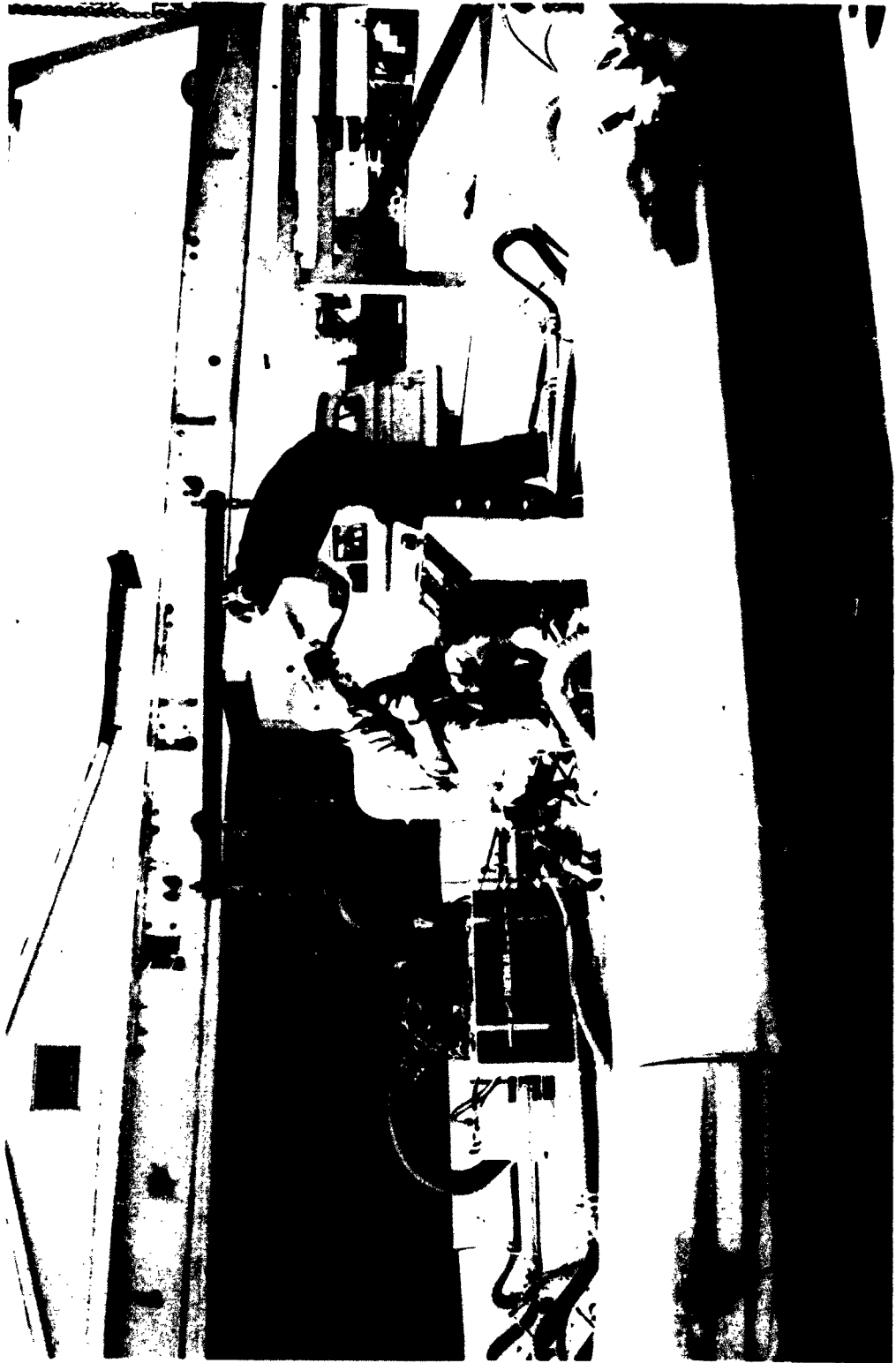


Figure 1. Preloaded on Overhead Support System

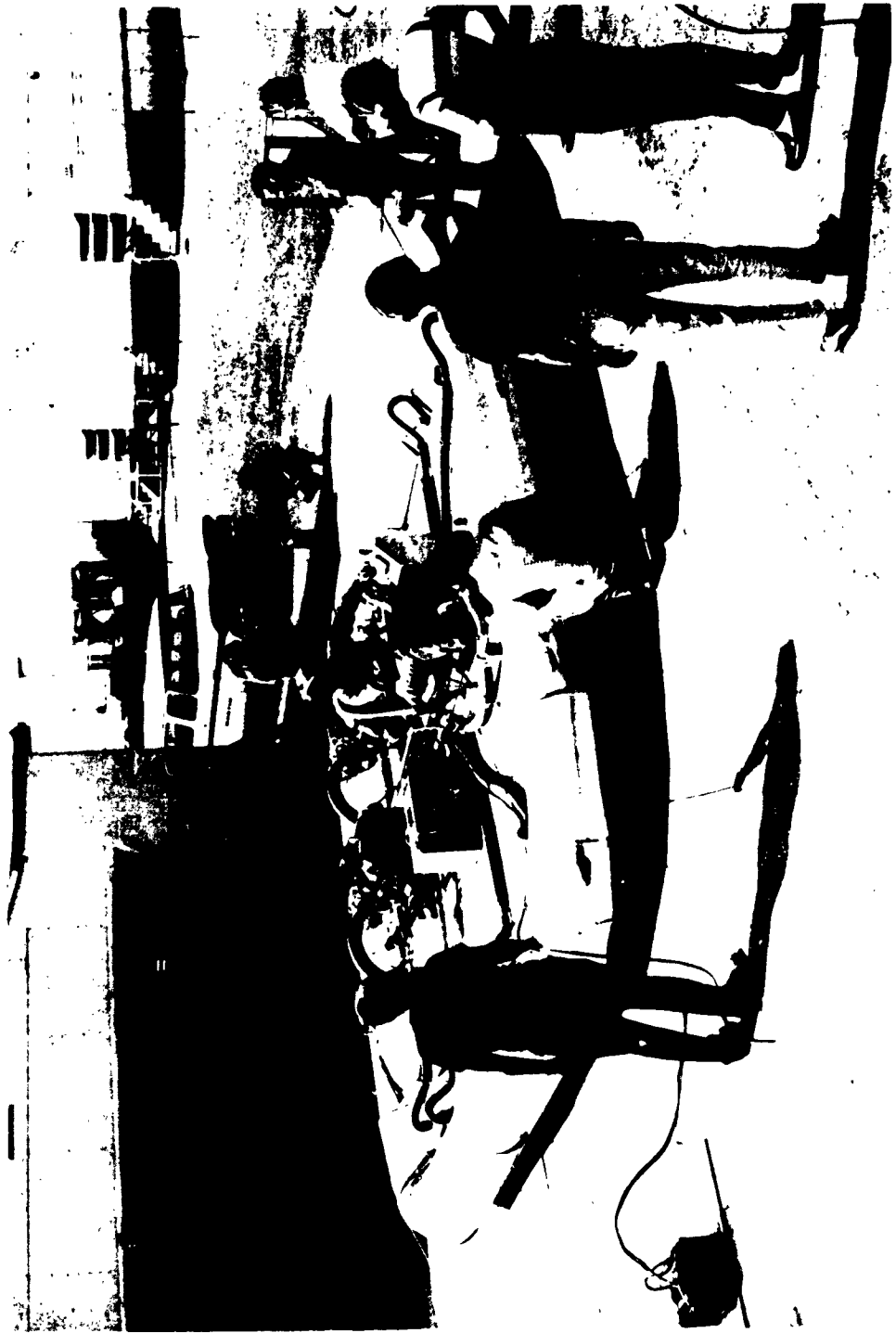


Figure 2. Initial Run-up of Engines



Figure 3. Tethered Hovering Tests

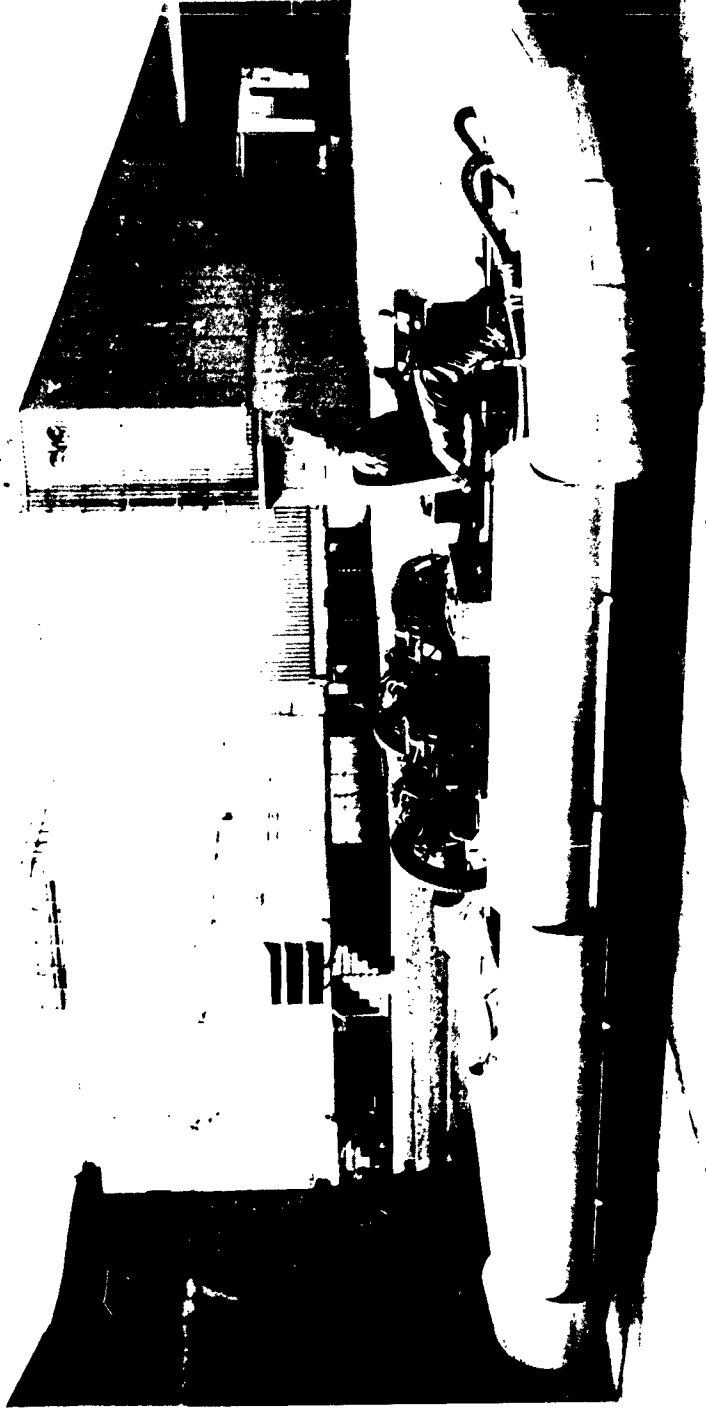
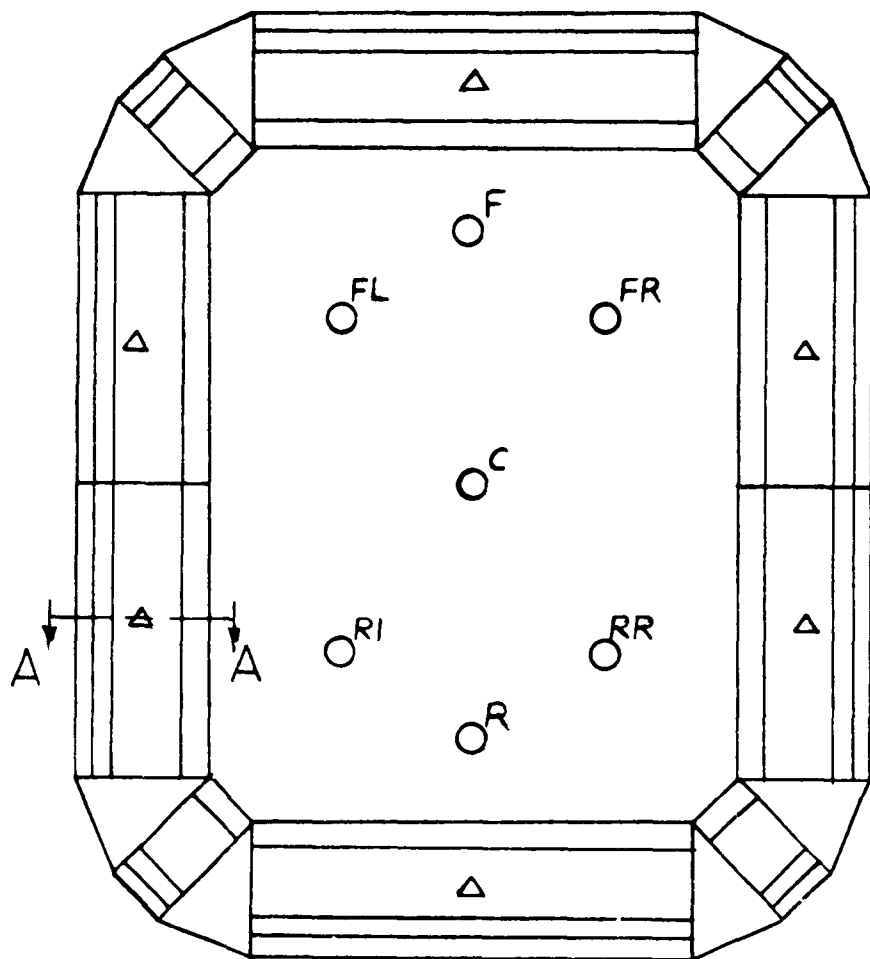


Figure 4. Evaluating Control Effectiveness




 CAVITY PRESS
TAP
SECTION A-A

○ BASE PRESSURE TAP
 △ CAVITY PRESSURE TAP

Figure 5. Base Instrumentation

PERFORMANCE

Engine Performance

The engines used to power the NCTV were two AiResearch Model GTC 85-24 bleed air engines. These engines were selected primarily because of their availability as GFE. Manufacturer's performance specifications are shown in Figure 6, where maximum bleed air flow, bleed pressure, and temperature are presented as a function of ambient temperature.

The ejector headers were sized for an 80°F ambient temperature. Thus a total bleed flow of 3.6 lb/sec at 430°F and 33 psig* was anticipated, yielding 320 air horsepower.

Considerable operational difficulties were encountered with both of the GTC 85-24 engines, ranging from fuel control malfunctions to a complete turbine failure requiring engine replacement.

While the test program was initiated at a time when 60 to 70°F ambient temperatures were prevalent, it soon became apparent that the GTC 85-24 engines would provide inadequate performance in 100 to 120°F ambient temperature, which might be expected during the summer months. Therefore, when the turbine failure occurred, the model GTC 85-72 engine was obtained as a replacement. At 120°F, the GTC 85-72 engines deliver 318 air horsepower to the ejectors, or slightly less power than was available from the GTC 85-24 engines at 80°F.

For reasons that are discussed in following sections, additional power was required to overcome ejector performance deficiencies. To this end, water injection at the compressor inlet was utilized to increase the bleed flow capability of the GTC 85-72 engines. Figures 7 and 8 present experimental data for water injection rates of 0 to 50 gallons per hour per engine. It is seen that a 50 gph injection rate increases bleed flow 22 percent at constant engine speed and exhaust gas temperature while reducing the bleed temperature 110 degrees and increasing the bleed pressure 2.7 psi. The net result is a 16 percent increase in air horsepower delivered to the ejectors.

Engine failure was experienced with one of the GTC 85-72 engines due to improper turbine assembly during overhaul. The GTC 85-72 turbine section was damaged beyond repair and was replaced, under the supervision of the manufacturer's service representative, with the turbine from the operable GTC 85-24 engine, and testing was continued.

* A maximum pressure drop of 2 psi in the ejector feed lines was anticipated.

100% BLEED LOAD
EGT = 1200°F

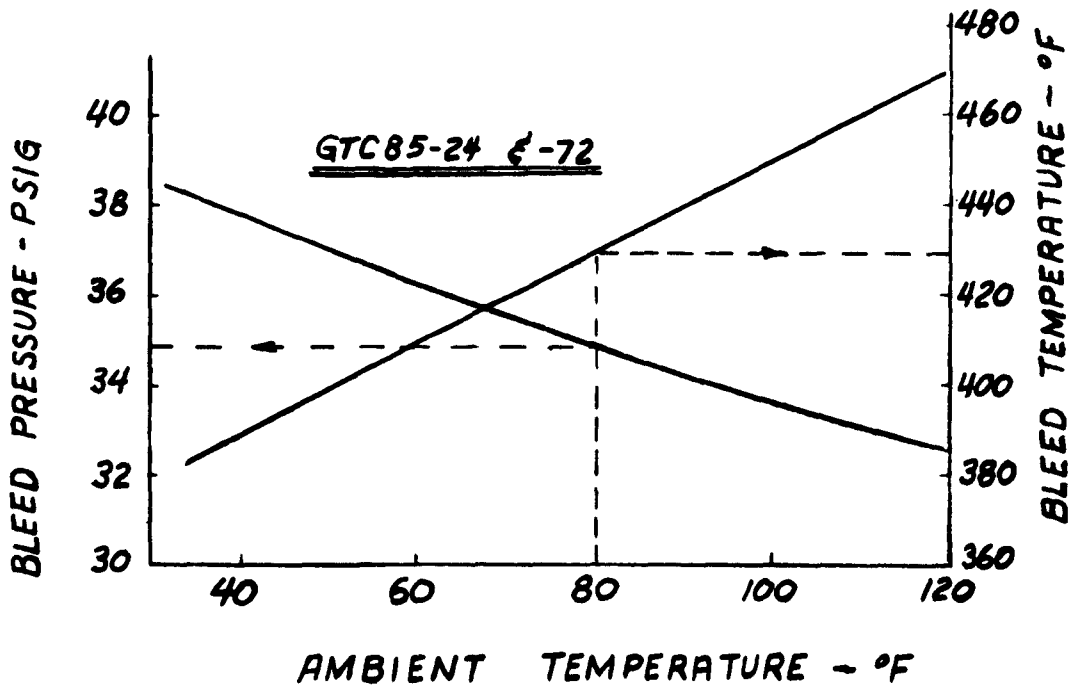
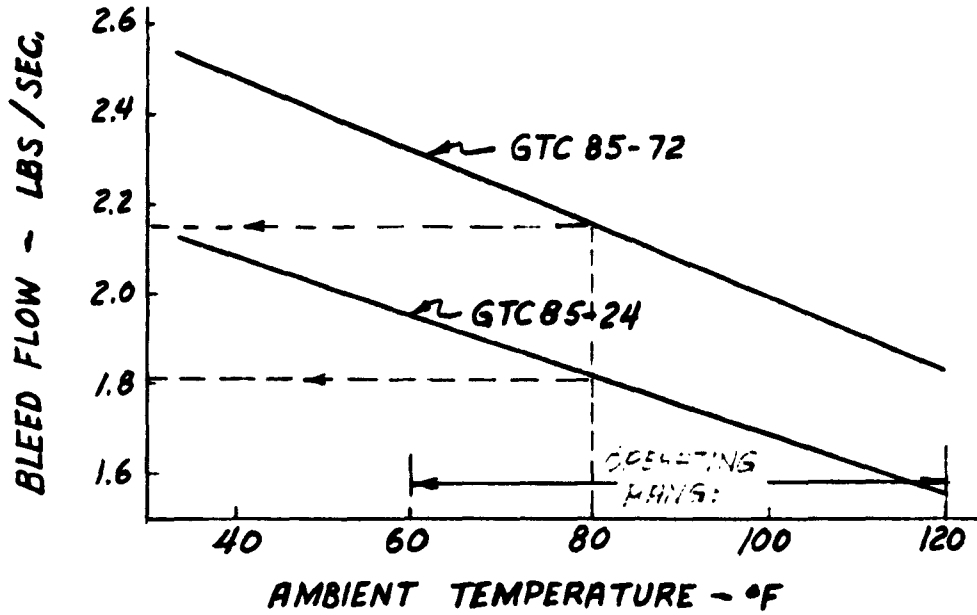


Figure 6. AiResearch Bleed Engine Performance

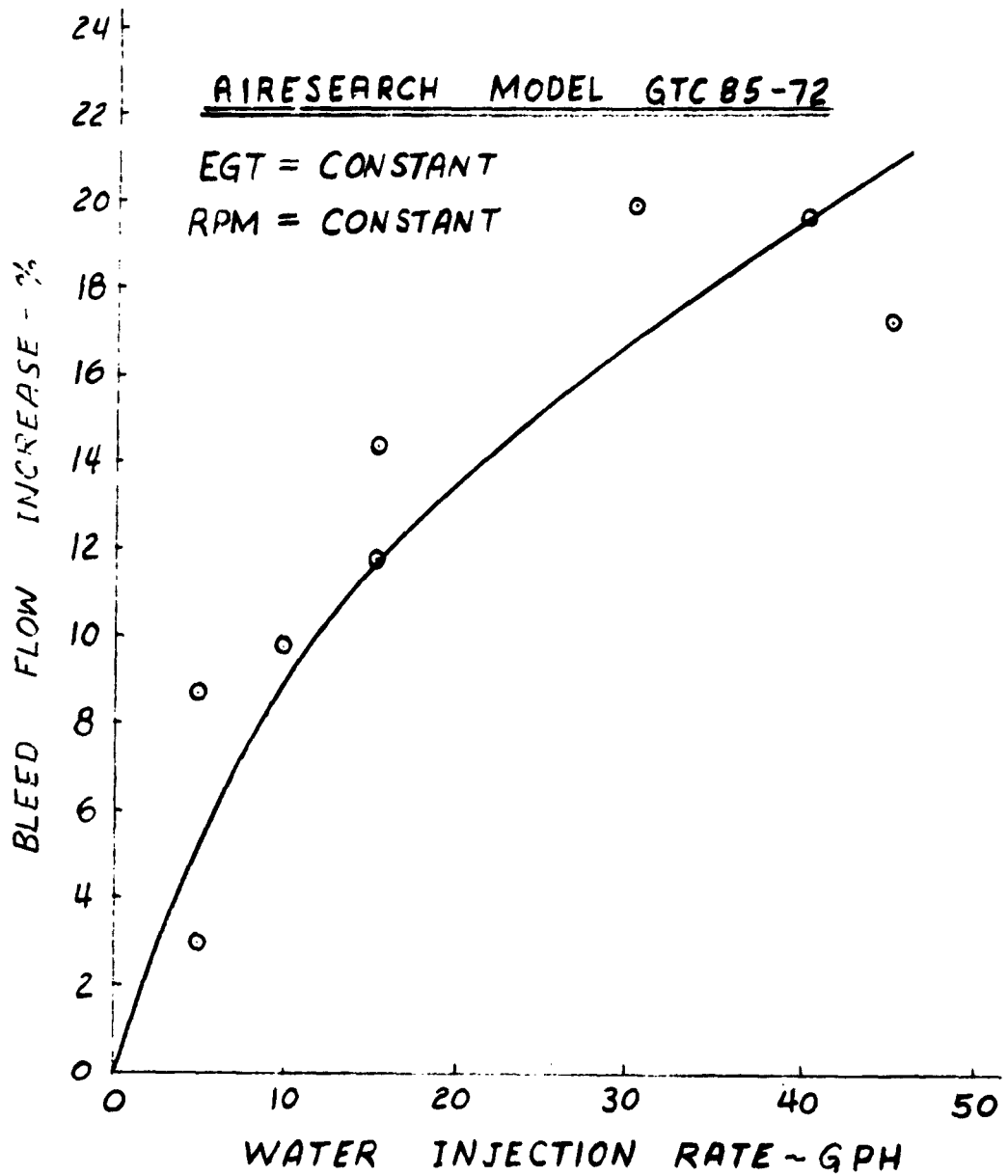


Figure 7. Effect of Water Injection on Bleed Flow

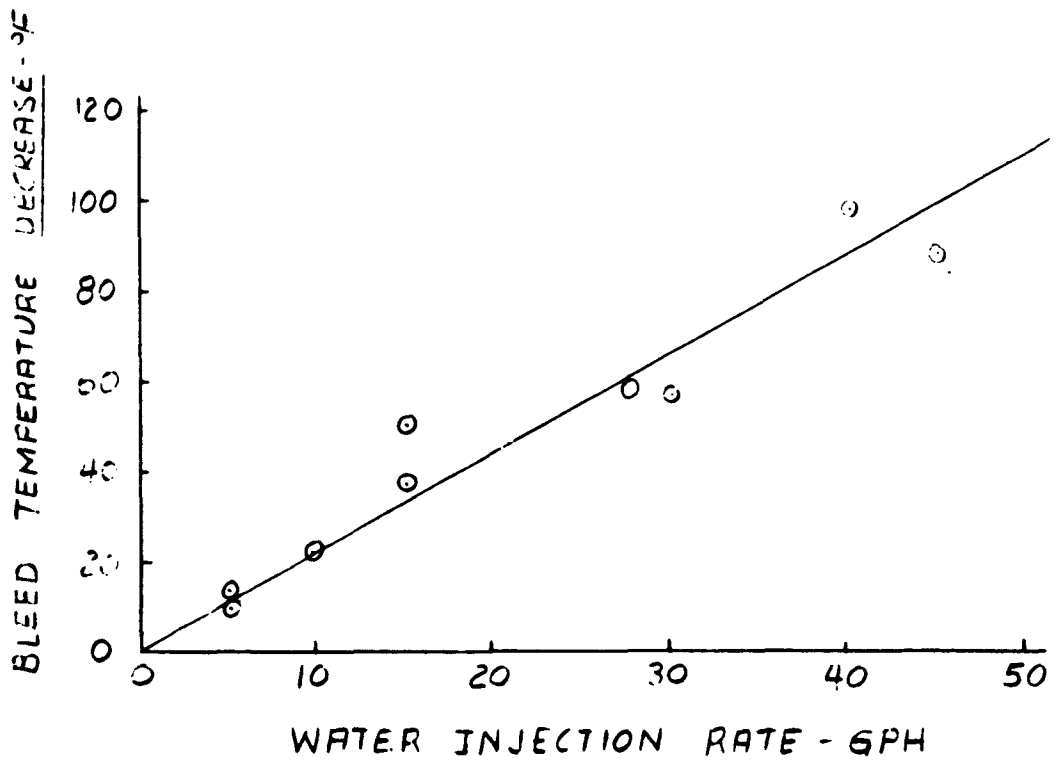
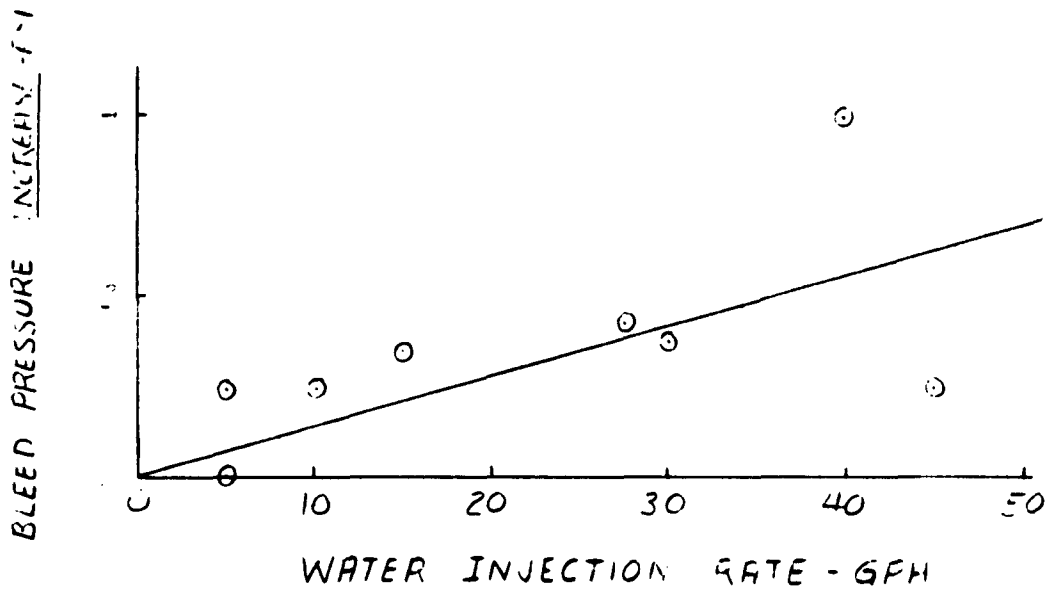


Figure 8. Effect of Water Injection on Bleed Temperature and Pressure

The test program was continually hampered by engine malfunctions and an inordinate amount of maintenance of the following types:

1. Corroded pneumatic control valves.
2. Intermittent operative fuel control valve.
3. Acceleration limiter malfunction.
4. Turbine speed governor malfunction.
5. Bleed load control valve contaminated.
6. Foam in oil sump, requiring baffling.
7. Fuel cracking pressure regulator improperly adjusted.
8. Defective electrical wiring.
9. Installation of heavy-duty filter in fuel line.

These problems were in part due to the necessity of operating the engine at maximum power and subjecting them to an abnormal number of starts.

Ejector Performance

A schematic identifying the various components of the ejector assembly is shown in Figure 9. Two-dimensional performance data on the basic ejector design, designated model 5, are presented in Figure 10. Although model 5 base pressure level fell short of design expectations, it appeared adequate to provide a 1-foot operating height on the vehicle, utilizing the available engines.

Upon completion of the first corner ejector for the MCTV, the configuration was tested in the 2-D facility. A 1 pound per square foot deficiency in base pressure generated by the corner ejector was evident and is attributed in part to manufacturing tolerances, i.e., the effect of rivet heads and other irregularities in the flow path that were not present in model 5.

Initial 3-D MCTV tests were conducted with the optimum flap settings as determined from the 2-D tests. The resultant 3-D base pressure level was far below expectations as shown in Figure 10.

The slope of the base pressure versus height curve indicates that flow attachment was being encountered above 10 inches. Compartmentation of the vehicle base to eliminate corner leakage and to simulate 2-D conditions resulted in a slight improvement in base pressure but still fell far short of required values. Adjustment of the ejector flaps significantly improved the simulated 2-D perfor-

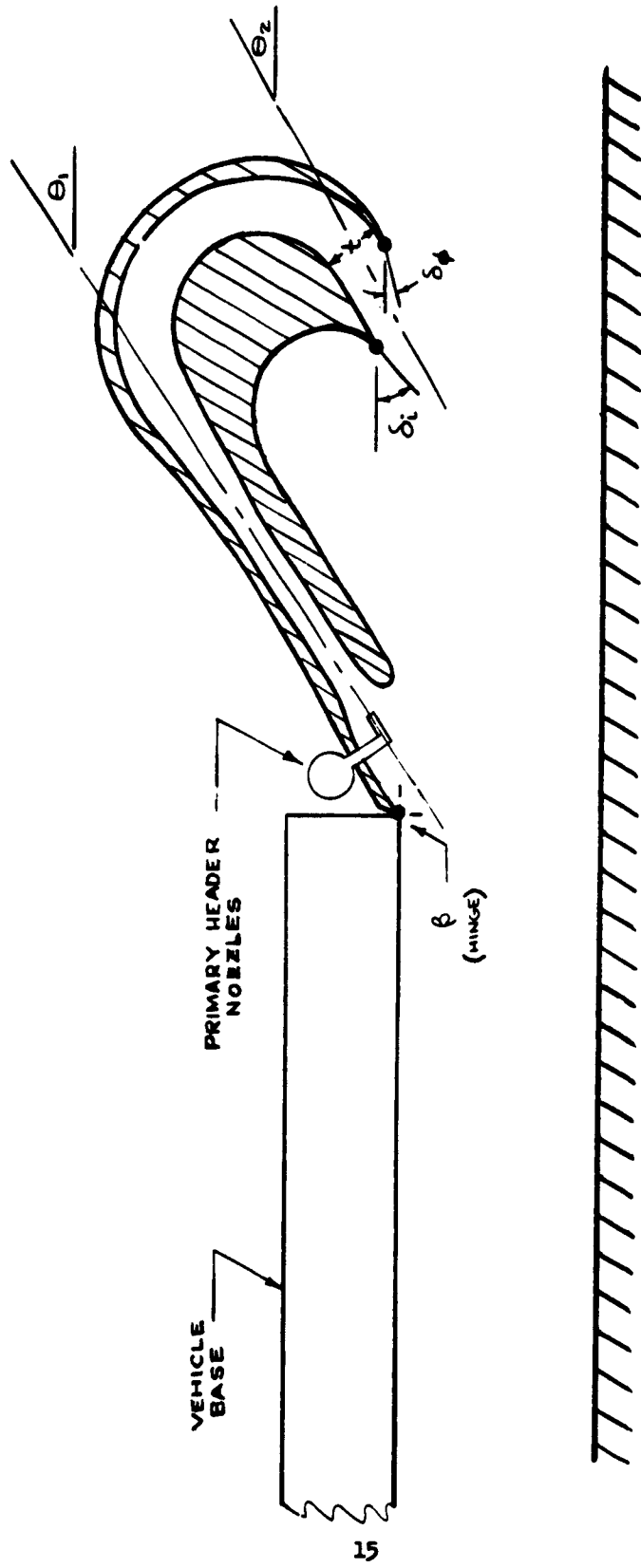


Figure 9. Schematic Ejector Components

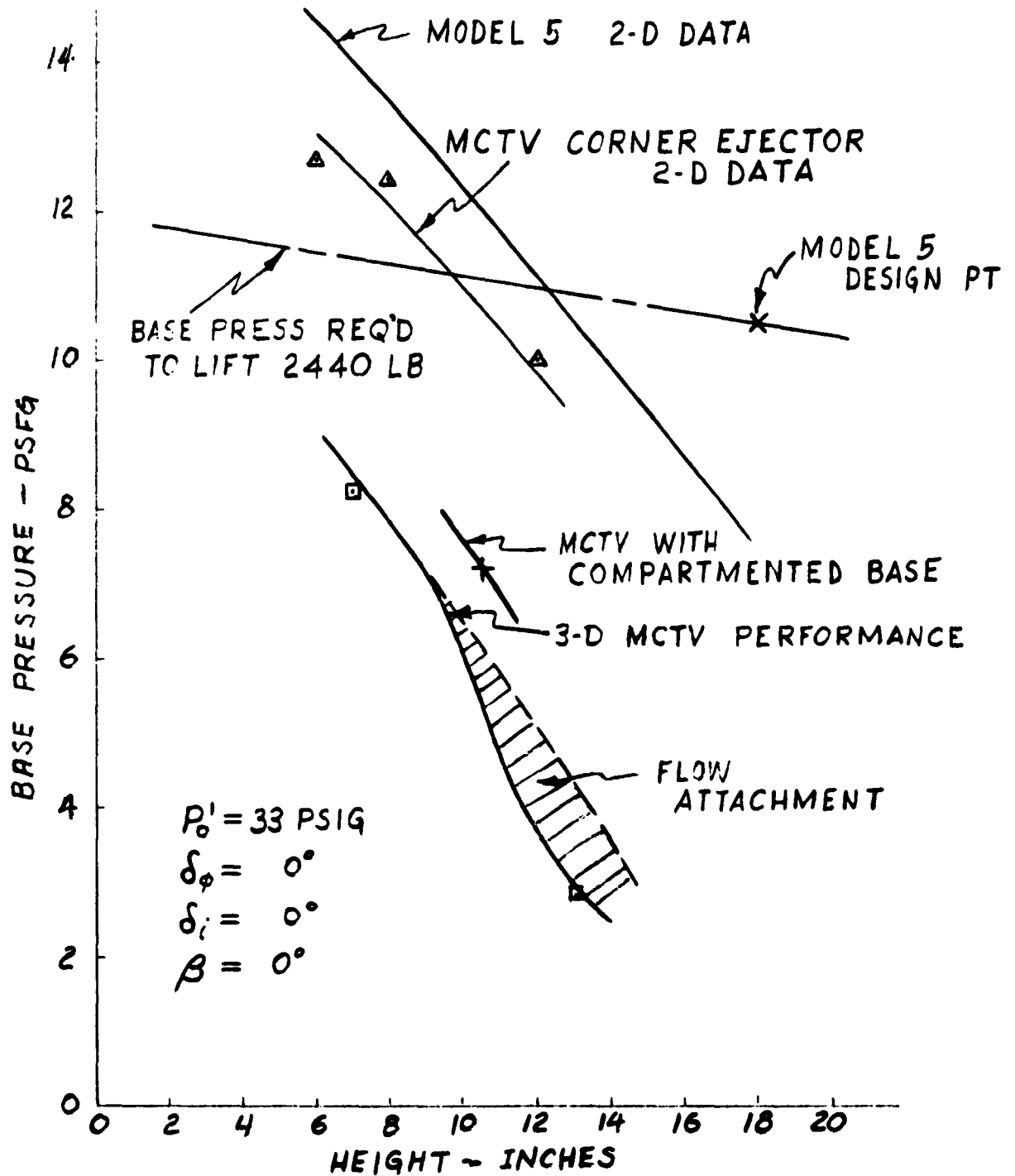


Figure 10. Comparison of 2-D and 3-D Base Pressure

mance as shown in Figure 11. However, the 3-D performance again fell significantly below 2-D levels.

The difference between MCTV compartmented base performance and the 3-D performance is believed to be largely the effect of corner leakage, although other phenomena such as curtain nonuniformities, etc., may be present. The 1 pound per square foot difference between 2-D corner ejector data and MCTV compartmented base data is not fully understood, although the combination of flap settings, required to prevent attachment, may introduce additional losses in the flow. Lower (more negative) cavity pressure level on the MCTV appears to contribute to this difference also.

The initial throat dimension of the header nozzles was slightly undersize, and the engines were not fully loaded as evidenced by exhaust gas temperatures of 1100°F while the engines are rated at 1200°F. Thus, 9 percent additional horsepower was available for the engines. This power was utilized by reaming the primary nozzles for a 22 percent area increase to accommodate the increased mass flow at lower pressure. The resultant base pressure level is shown in Figure 12. The additional power was converted to base pressure as evidenced by the agreement between prediction and test data. The resultant 3-D base pressure level permitted a hovering demonstration at minimum gross weight. This demonstration was made with an ambient temperature of 60°F and a gross weight of 2250 pounds. The increased engine output under the 60°F ambient temperature raised the 3-D base pressure level sufficiently to permit hovering at a 9 to 10 inch height. The demonstration was of short duration because of an engine malfunction but did prove the feasibility of containment of the pressurized base air with a recirculating curtain.

In light of the different flap settings required to obtain satisfactory 3-D performance, a systematic optimization of the flaps in the 3-D configuration was undertaken. These data are presented in Figures 13 through 17. It is apparent that the optimum flap settings are 0 to 10 degrees for the outer flap and 60 degrees for the inner flap. These settings result in the greatest range of heights over which acceptable performance is realized. It will be noted that with the inner flap at 60 degrees, the outer flap setting is not critical. The effect of the inner flap is to prevent or delay flow attachment and has a very marked effect on base pressure at high heights. The outer flap is not as effective in controlling flow and apparently is primarily effective through throttling action on the ejector flow.

It is interesting to observe how the optimum flap settings vary with height as shown below:

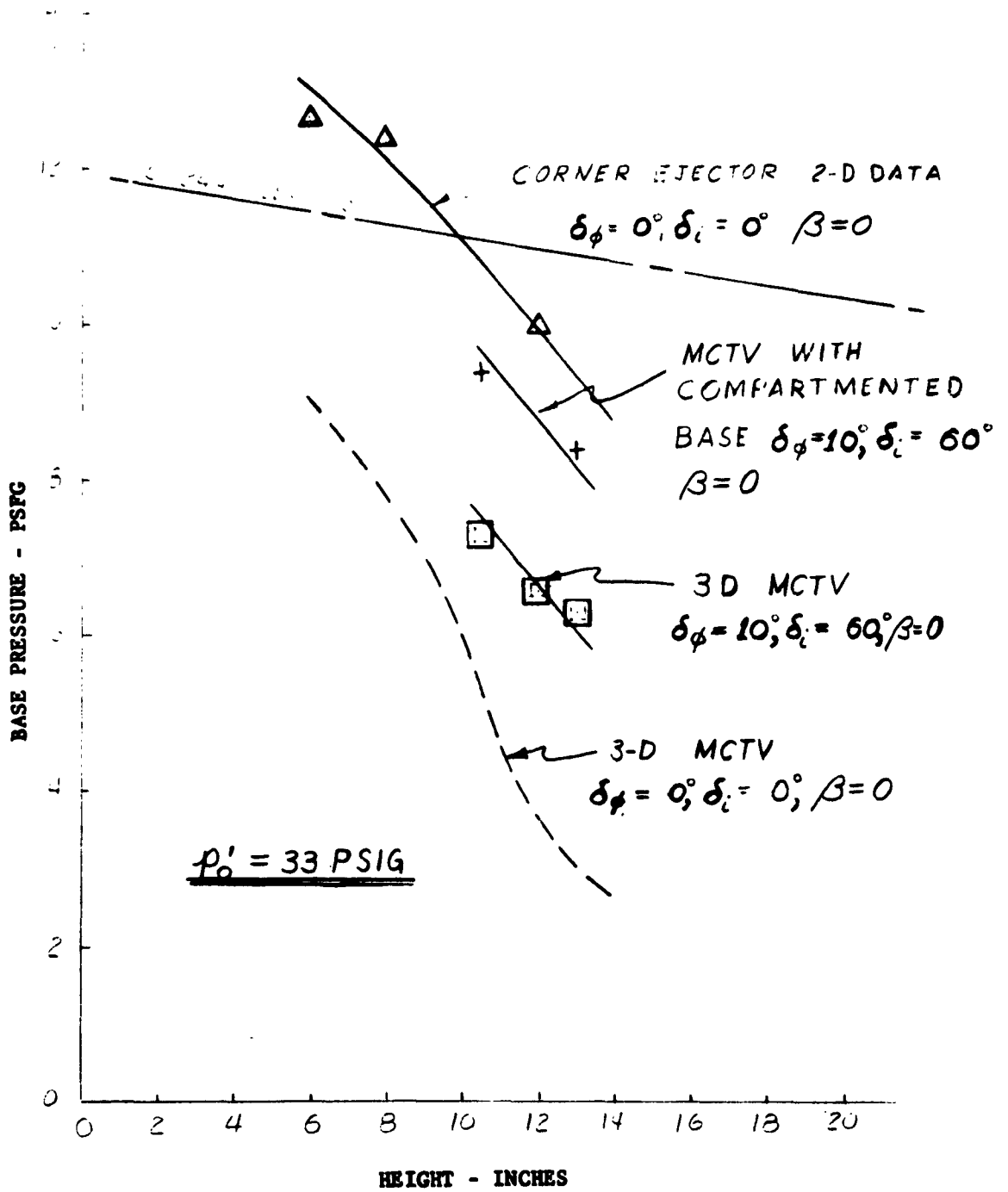


Figure 11. Comparison of 2-D and 3-D Base Pressure

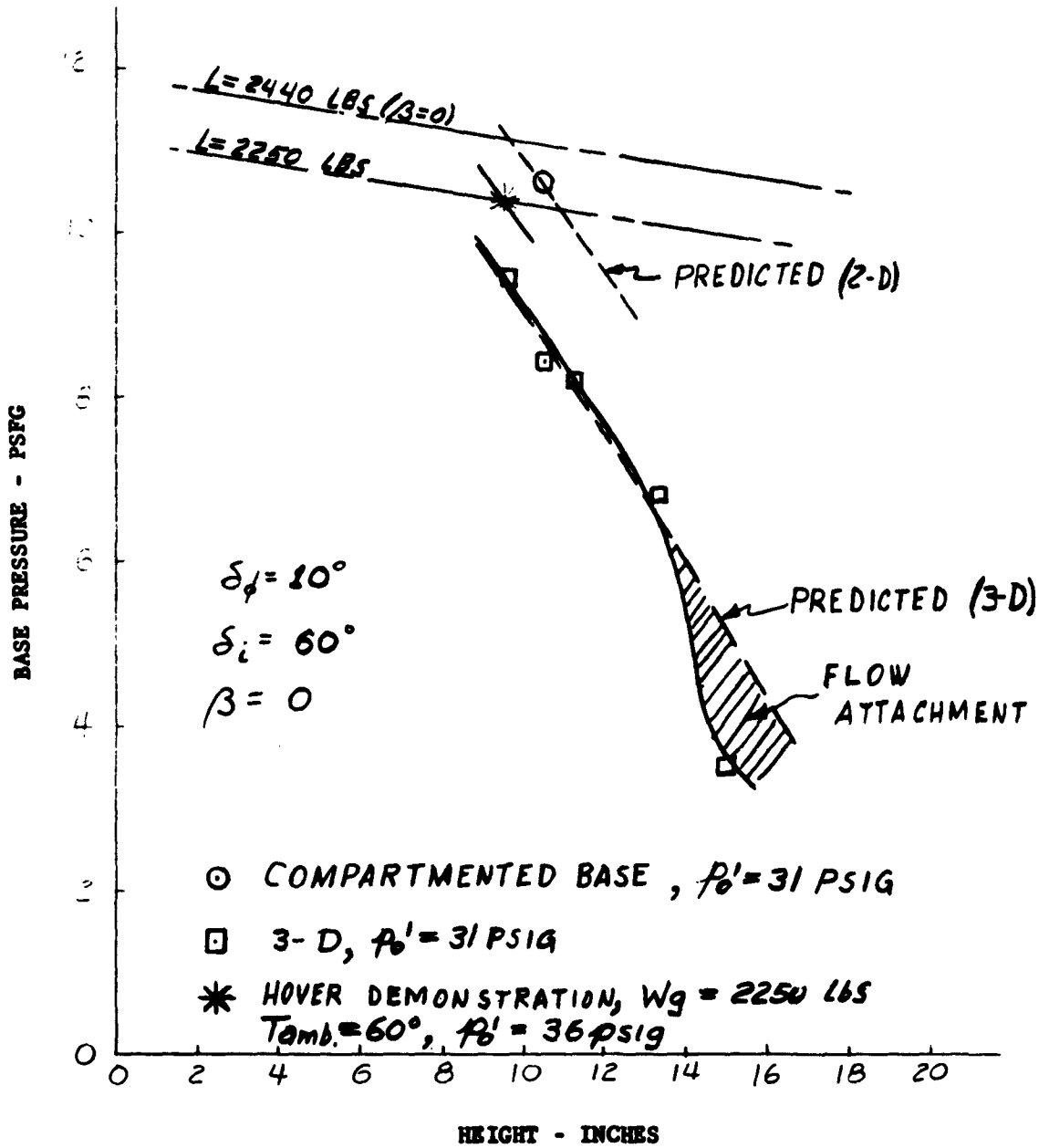


Figure 12. Effect of Increased Primary Mass Flow on Base Pressure

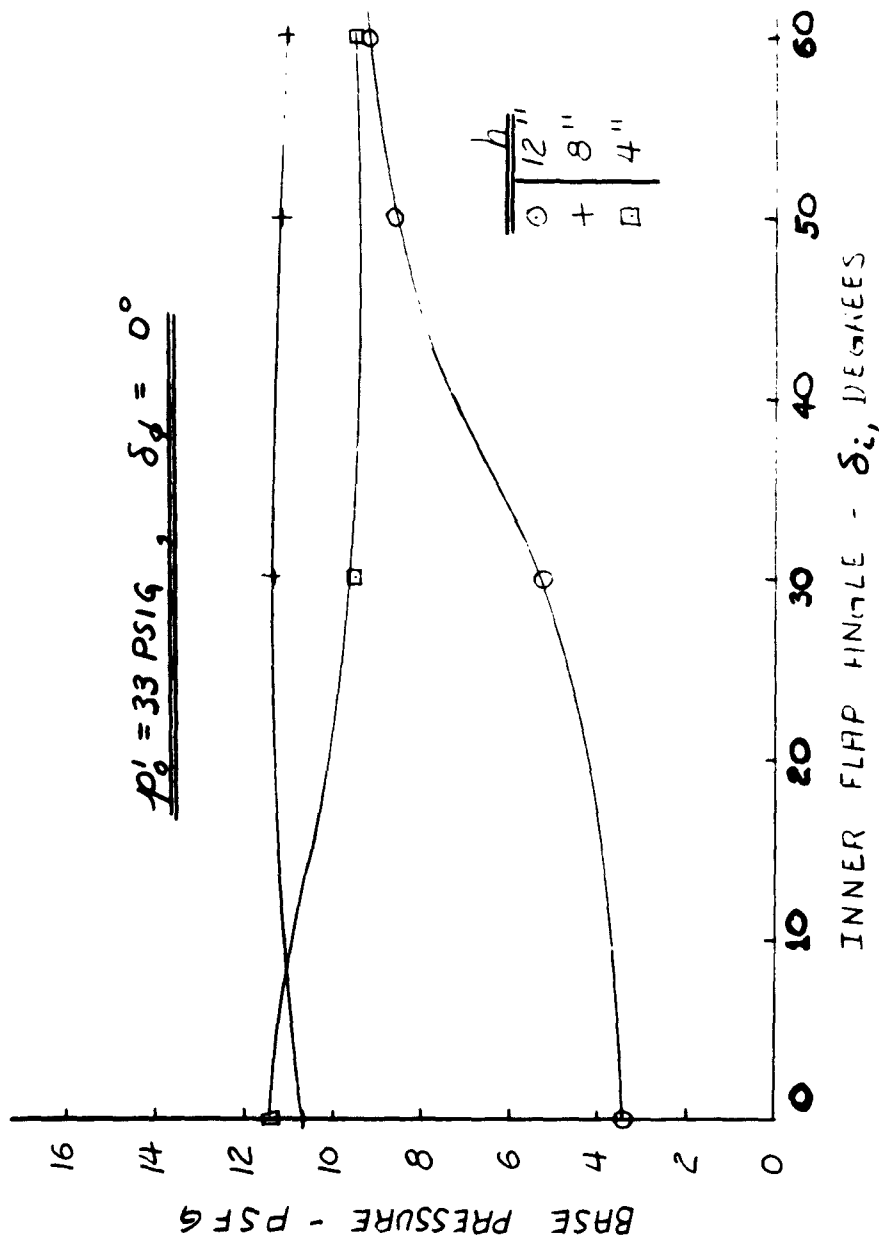


Figure 13. Effect of Inner Flap Setting on Base Pressure

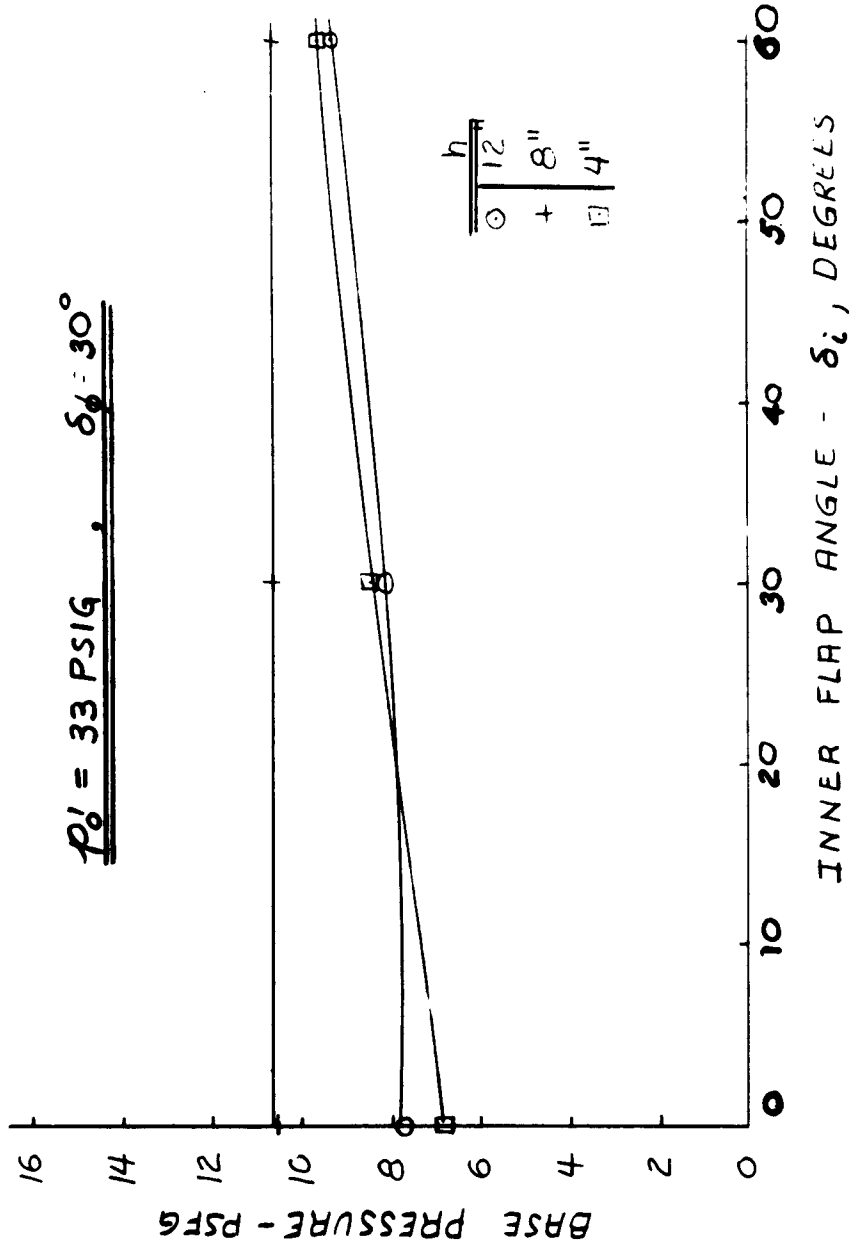


Figure 14. Effect of Inner Flap Setting on Base Pressure

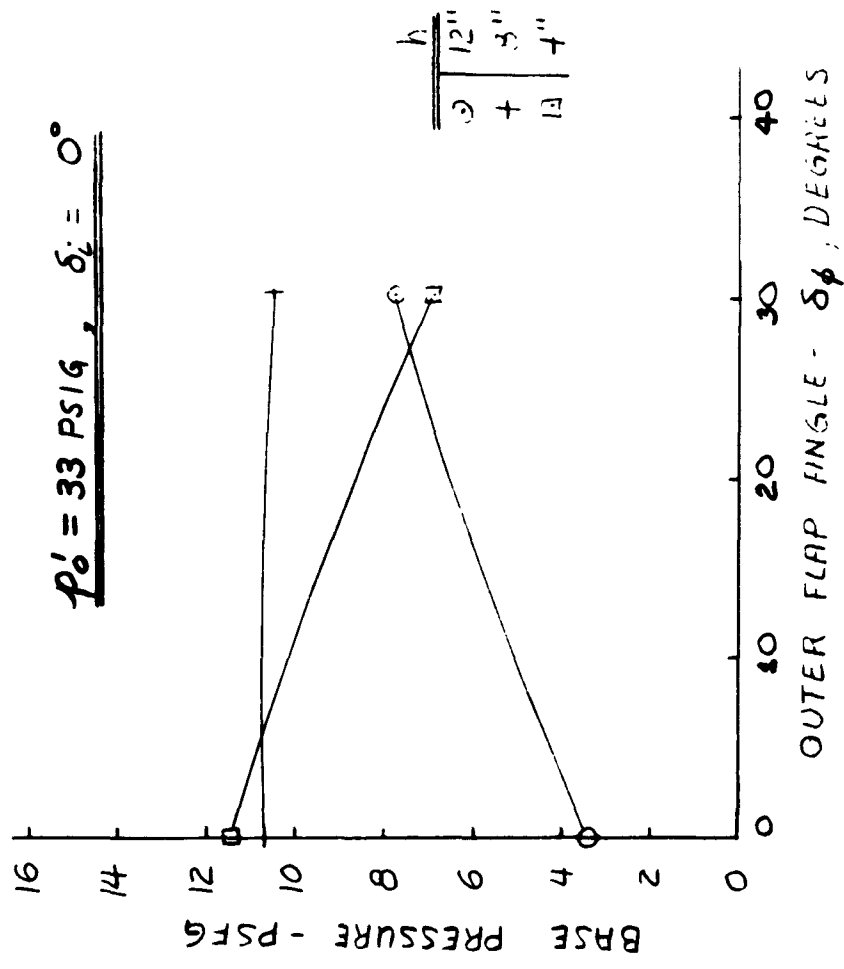


Figure 15. Effect of Outer Flap Setting on Base Pressure

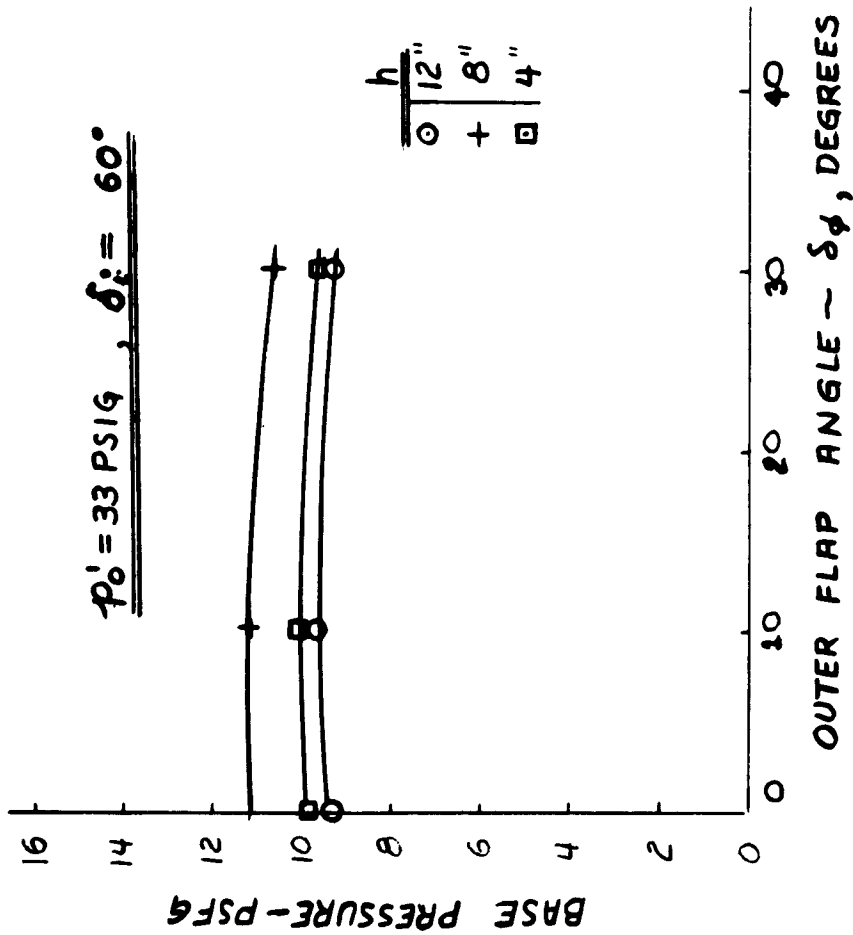


Figure 16. Effect of Outer Flap Setting on Base Pressure

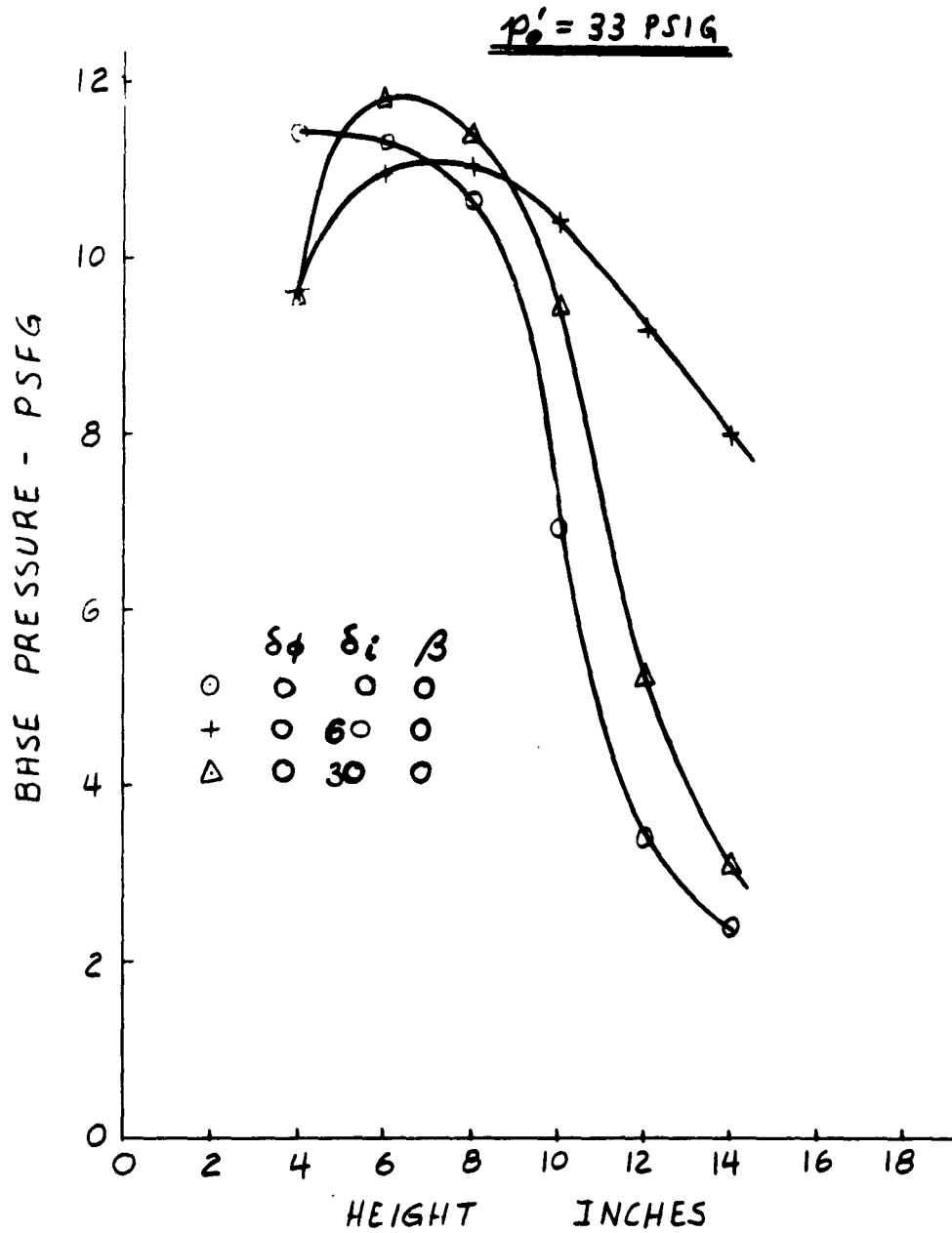


Figure 17. Effect of Ejector Flap Angles on Base Pressure

height (inches)	δ_o opt	δ_i opt
4	0	0
8	0	30
12	0	60

It is apparent that a smooth variation of the inner flap setting from 0 degrees at a height of 4 inches to 60 degrees at 12 inches would provide optimum performance at all heights. While the influence of the flaps on ejector performance is not completely understood, some general observations concerning their effect may be made. The ejector overhang dimension was determined by the design height of 18 inches. This overhang dimension, together with the nominal exit angle of 30 degrees, assured the jet of impinging on the ground prior to curving upward to the ejector inlet, thus containing the high-pressure base air.

At heights lower than the design height, it is apparent that the exit jet must curve inward due to the close proximity of the ground. This curvature of the outer jet severely reduces the cavity pressure and thus limits the base pressure that can be generated by the inner jet. These effects are shown graphically in Figures 18 and 19.

The effects of flaps at lower than design height are to direct the flow so that curvature of the outer jet is minimized and near-zero cavity pressure is maintained.

As shown in Figure 20, a similar problem can occur at greater than design height. The suction effect of the ejector inlet is such that at some height, the outer jet is pulled back into the inlet before it impinges on the ground. This results in negative cavity pressures and reduced base pressure since the base is sealed only by the comparatively weak primary jet in a manner similar to an annular jet.

The flow attachment phenomenon was not encountered at these heights in 2-D tests of model 5 ejector and is apparently a three-dimensional flow problem, although it may well be associated with the corner leakage present during these tests.

Figure 21 shows the effect of uniform ejector tilt on base pressure. Two different flap settings are shown for the case of upward tilt (negative β). The flap settings relative to the ejectors were held fixed as β was varied, therefore, the absolute exit angles changed as β was changed. For the zero degree inner flap setting ($\beta = 0$), the effect of tilting the ejectors up is to cause flow attachment, and subsequent loss in base pressure, to occur at a lower height. With the inner flap at 60 degrees ($\beta = 0$), upward ejector tilt causes a very slight loss in base pressure in the 10 to 14 inch height range while the effect at lower heights is insignificant. The

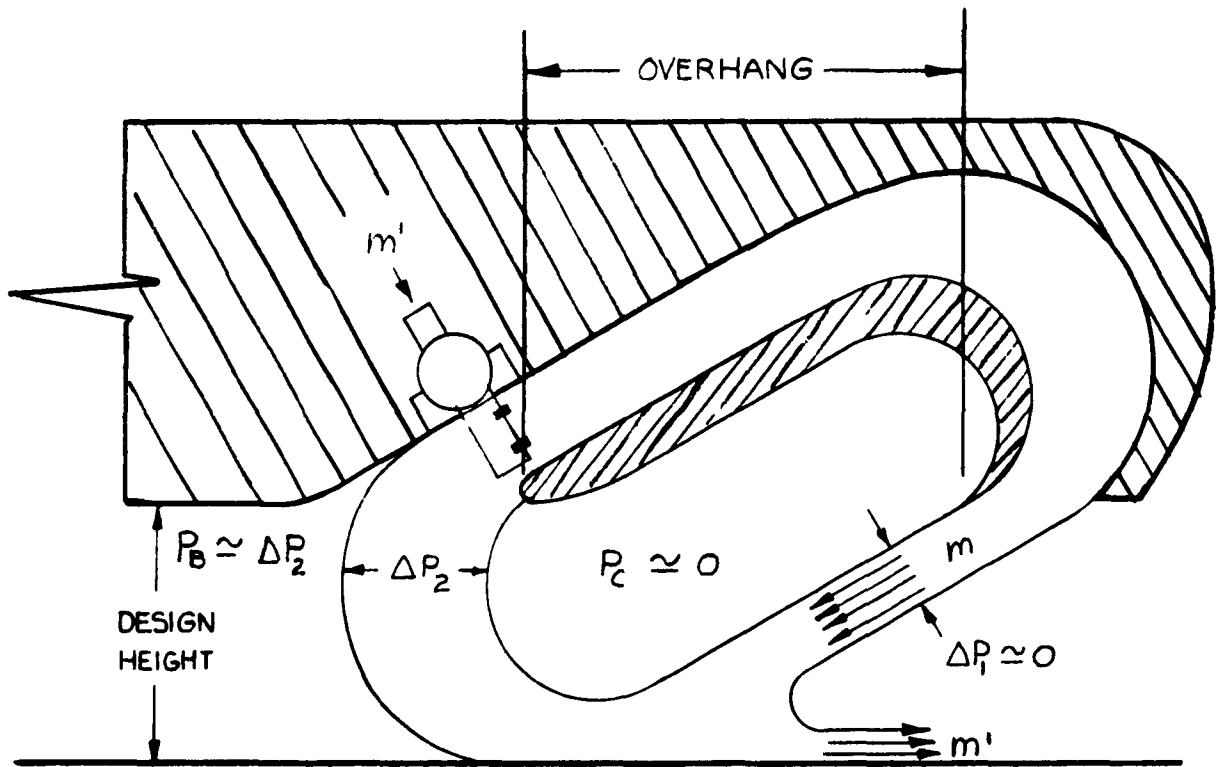


Figure 18. Recirculating Ejector Flow at Design Height

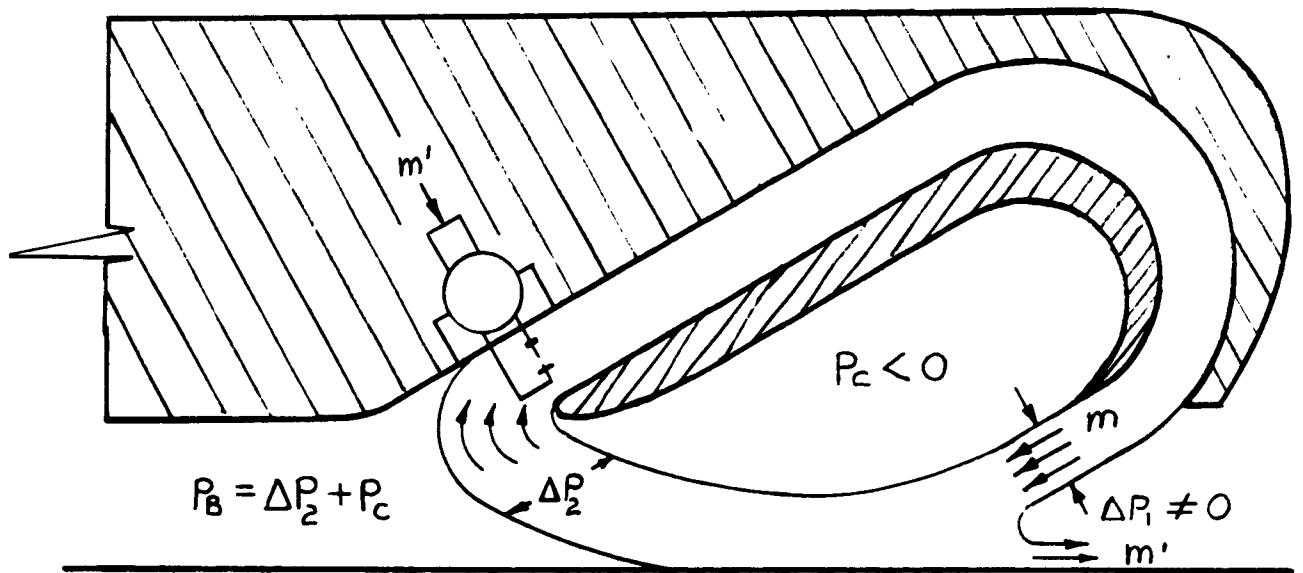


Figure 19. Recirculating Ejector Flow at Lower than Design Height

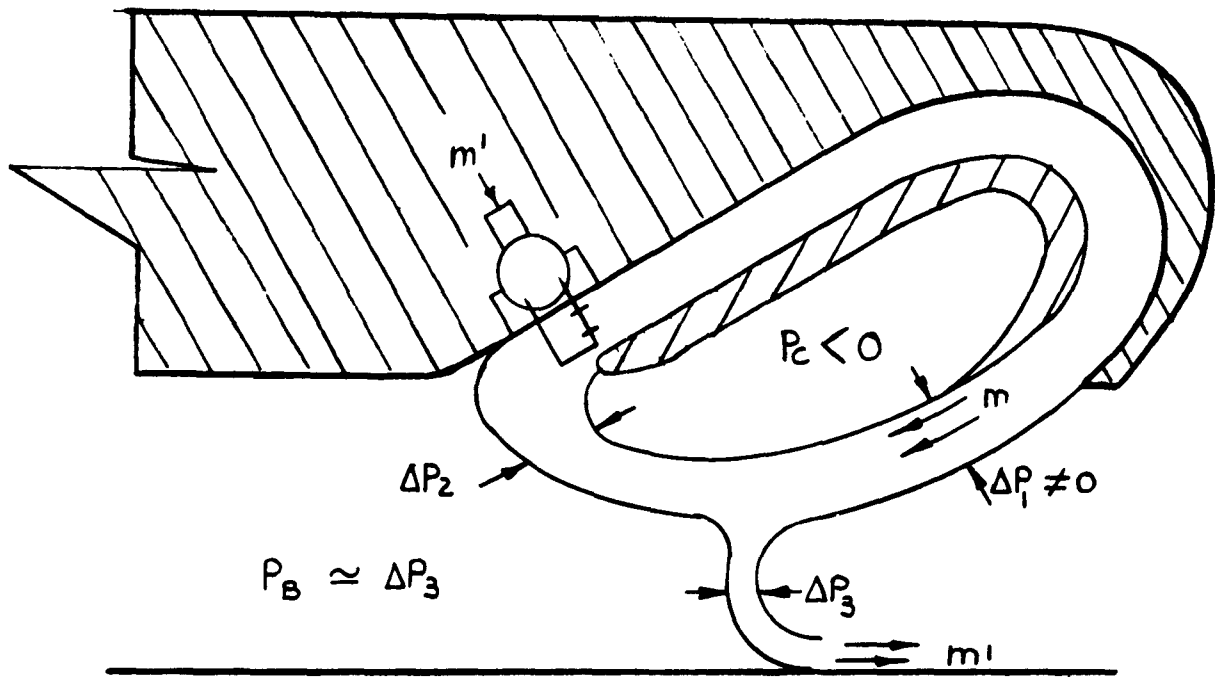


Figure 20. Recirculating Ejector Flow at Greater than Design Height

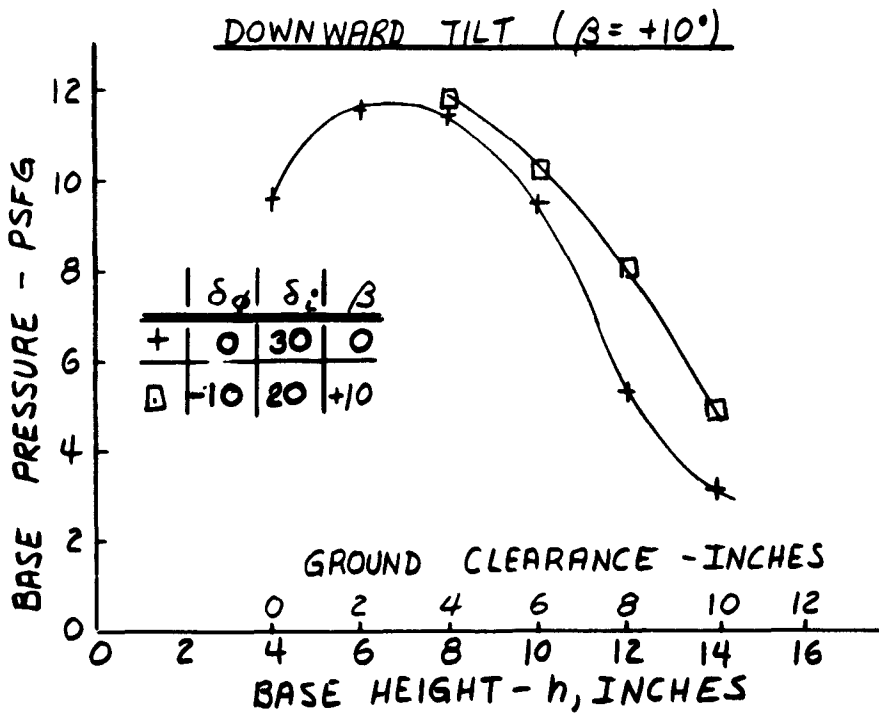
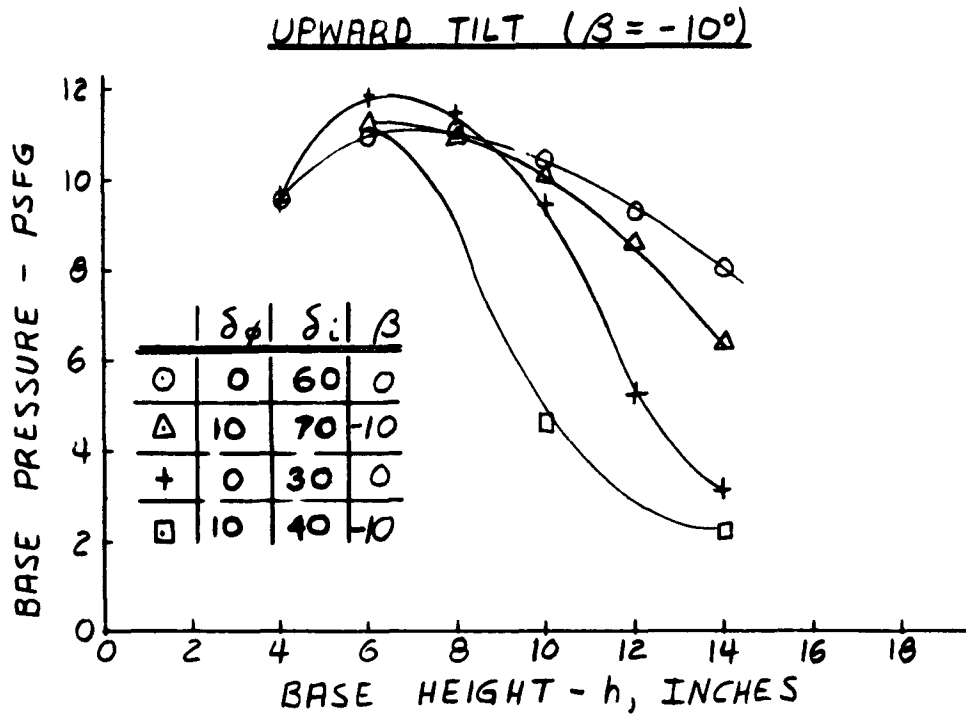


Figure 21. Effect of Uniform Ejector Tilt on Base Pressure

effect of downward tilt ($+\beta$) is just the opposite except that the ground clearance is reduced so that the net effect is a loss in base pressure if plotted against ground clearance.

Since the effect of upward tilt on base pressure is very slight for detached flow, the other beneficial effects appear to predominate. The benefits consist of increased momentum lift and maintenance of base clearance with full control deflection.

The variation of cavity pressure with height is shown in Figure 22. These data indicate that the level of cavity pressure is more negative than anticipated, accounting for some loss in lift capability and explaining in part the lower base pressure level, since the pressure jump across the inner jet is relatively constant and base pressure level follows cavity pressure directly.

Figure 23 shows the base pressure level obtained with water injection in the inlet of the gas turbines. This level appeared adequate to lift the vehicle to a height of 10 to 11 inches, and represents the configuration used to conduct hovering and forward flight tests. Water injection was effective in maintaining engine bleed output, hence, base pressure. With ambient temperatures as high as 120°F without water injection, the normal engine performance deterioration reduced base pressure below the level required for lift-off.

Hovering tests were conducted at minimum and maximum gross weights of 2200 and 2440 pounds respectively. Unfortunately, the stability and control aspects were so poor that little performance data could be obtained. Several hovering flights of short duration at 10 to 11 inches were made where wind gusts or other disturbances would cause one or more landing gear to contact the ground. Recovery through use of controls was only partially effective.

It was observed that lift-off was not accomplished over a grass surface or from an asphalt surface with exposed crushed rock of approximately 3/4 inch size. A measurement of base pressure over the asphalt surface indicated a 20 percent reduction from measurements on smooth concrete as shown in Figure 24. This phenomenon can only be explained by a loss in pressure recovery external to the ejector or by flow attachment. Apparently the turbulence set up by the surface roughness was sufficient to dissipate the energy of the curtain and prevent recovery of this energy at the ejector inlet. Subsequently, 2-D tests were conducted to determine the effect of surface roughness at various base pressures and heights. Figures 25 and 26 indicate that the loss in base pressure tends to be a constant amount rather than a constant percentage with regard to the recirculating air curtain strength. It is therefore anticipated that losses due to surface roughness will be relatively small for base pressure in excess of 35 pounds per square foot.

At this point it was apparent that forward flight was impractical both from the stability and control and from performance standpoints. Subsequent tests with castering wheels which supported approximately

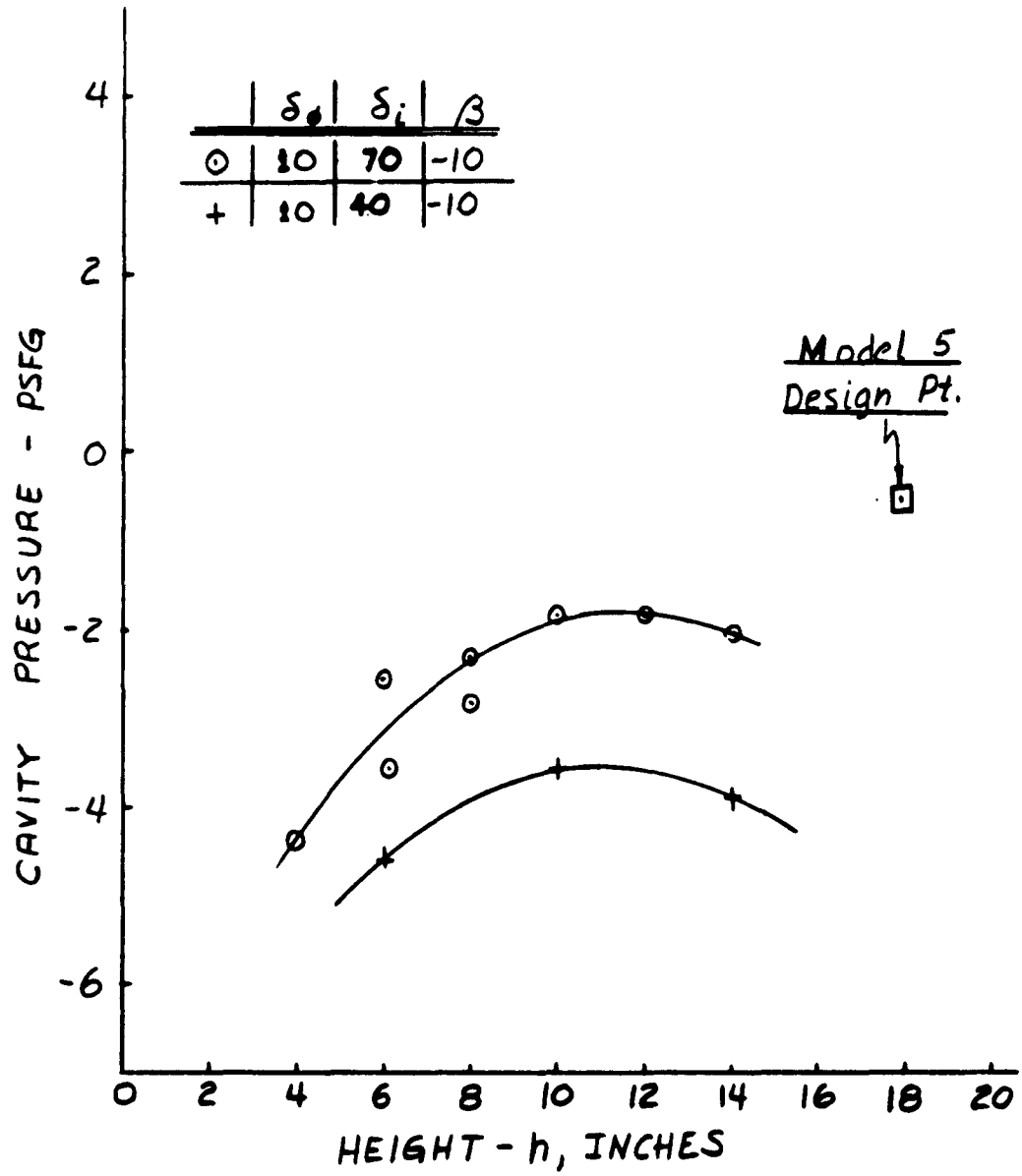


Figure 22. Cavity Pressure Variations with Height

$$\delta_d = 10^\circ \quad \delta_c = 70^\circ \quad \beta = -10^\circ$$

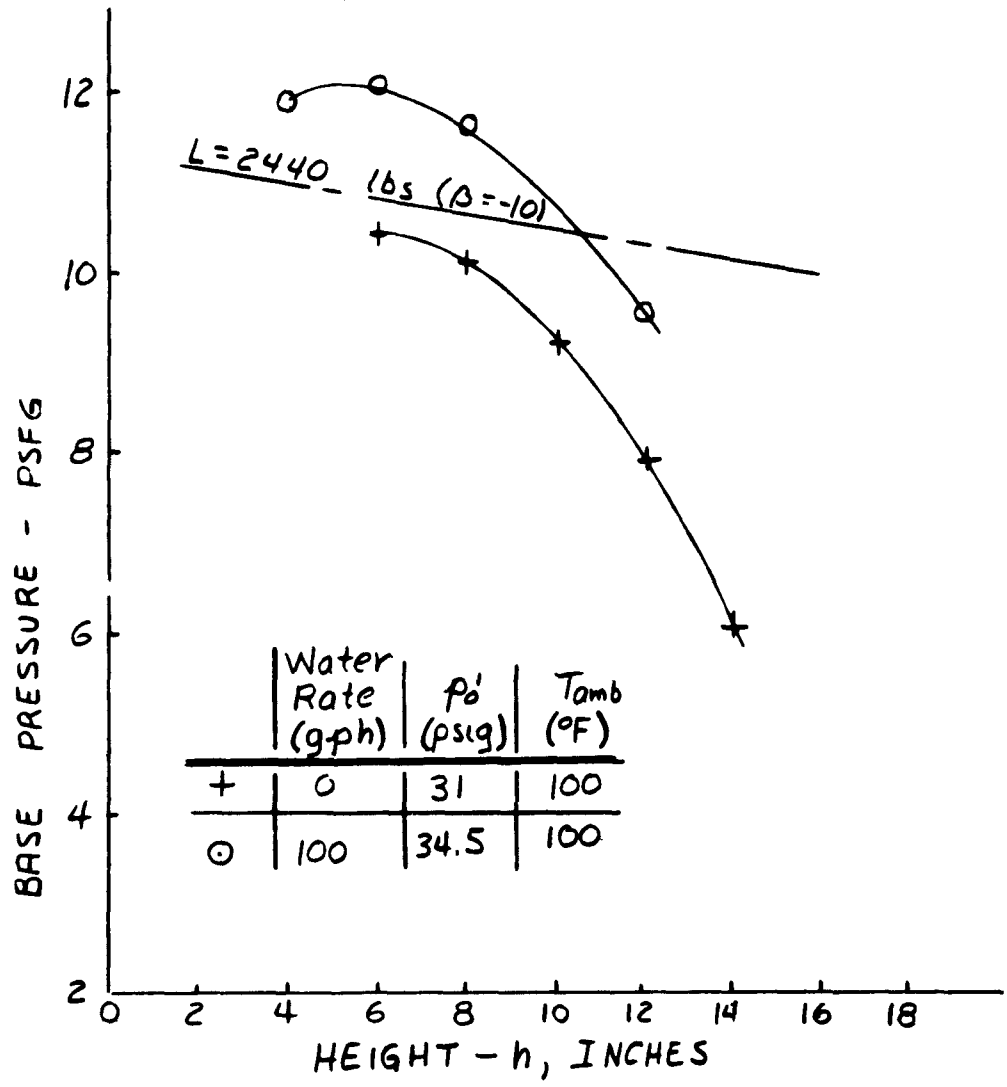


Figure 23. Effect of Water Injection on Base Pressure

$p'_0 = 34 \text{ psia}$ $\delta_d = 10^\circ$ $\delta_i = 70^\circ$ $\beta = -10^\circ$

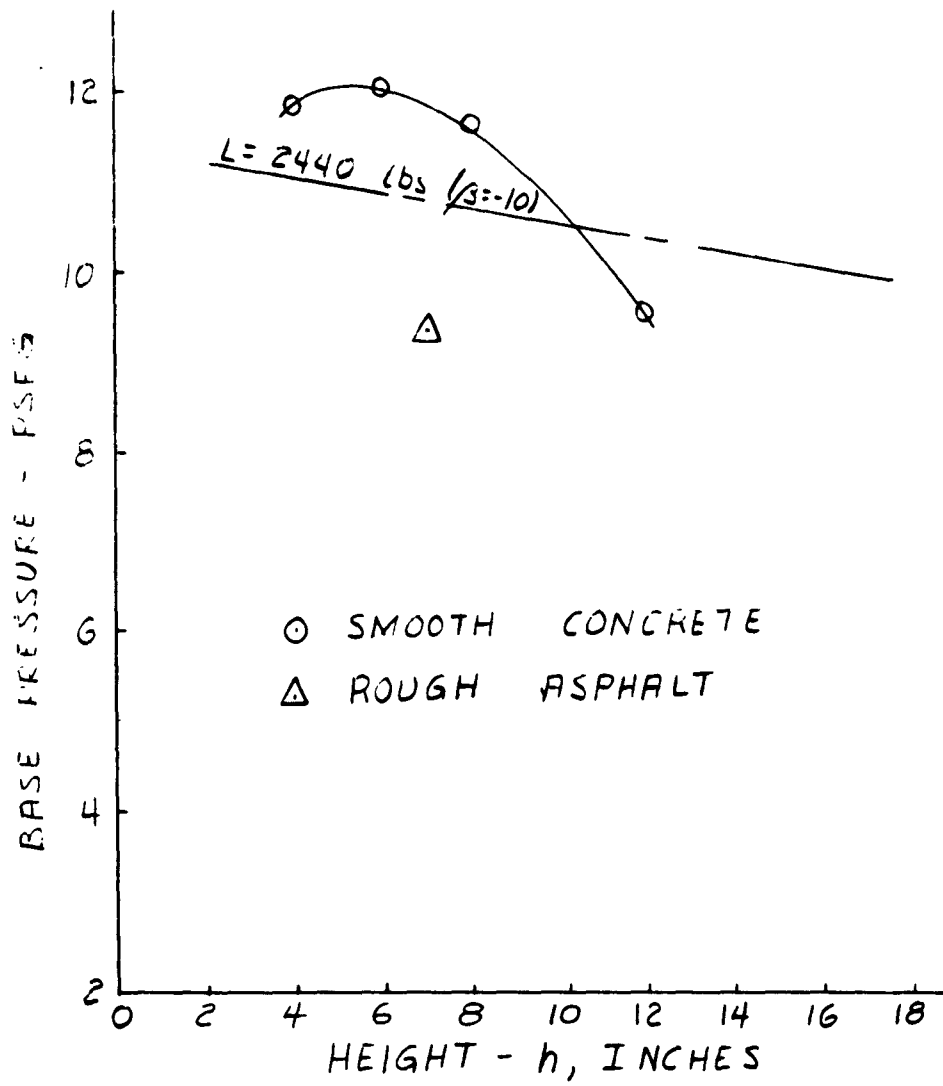


Figure 24. Effect of Surface Irregularity on Base Pressure

HEIGHT = 9 INCHES

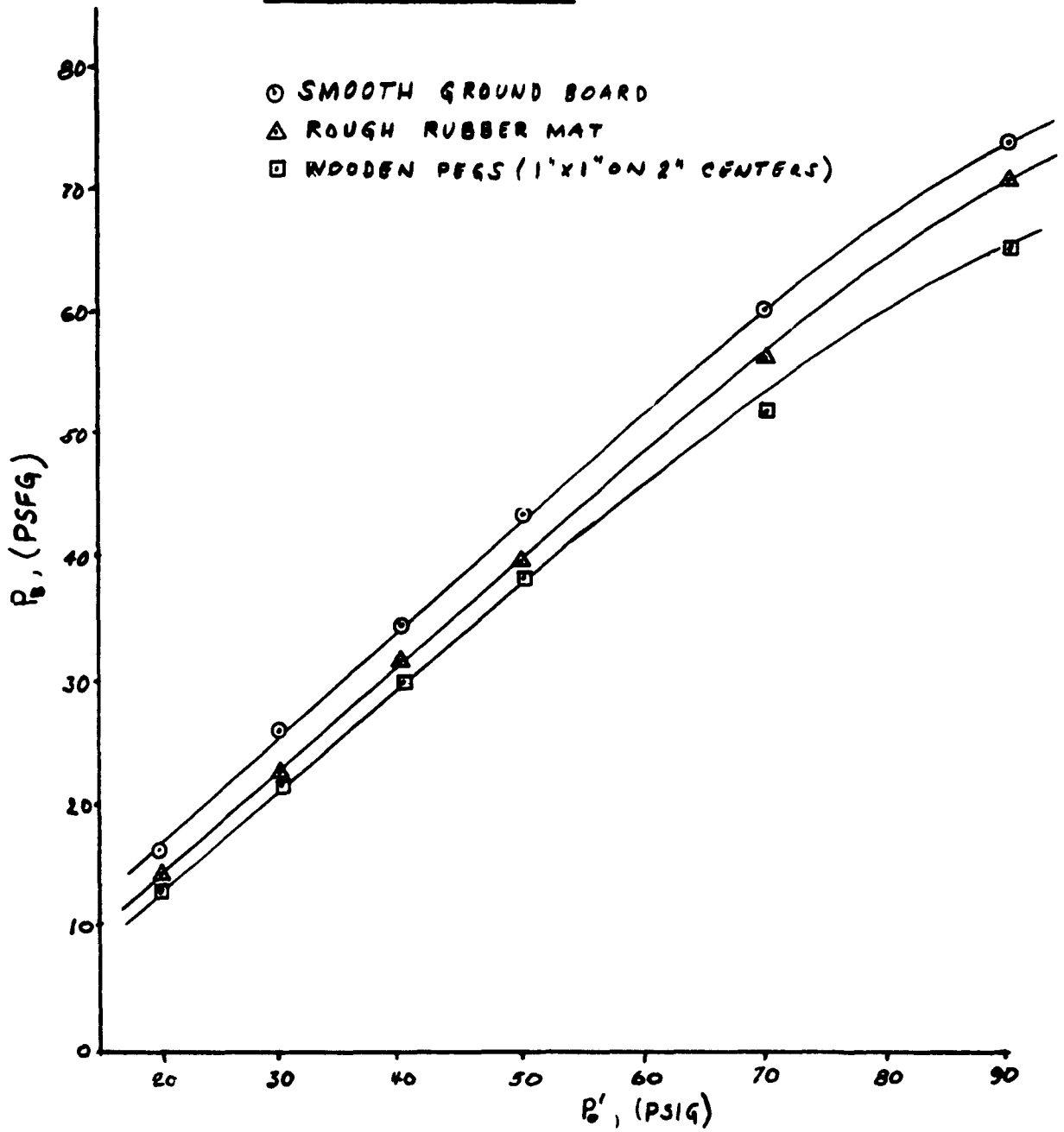


Figure 25. Effect of Surface Roughness for 2-D Tests

HEIGHT = 18 INCHES

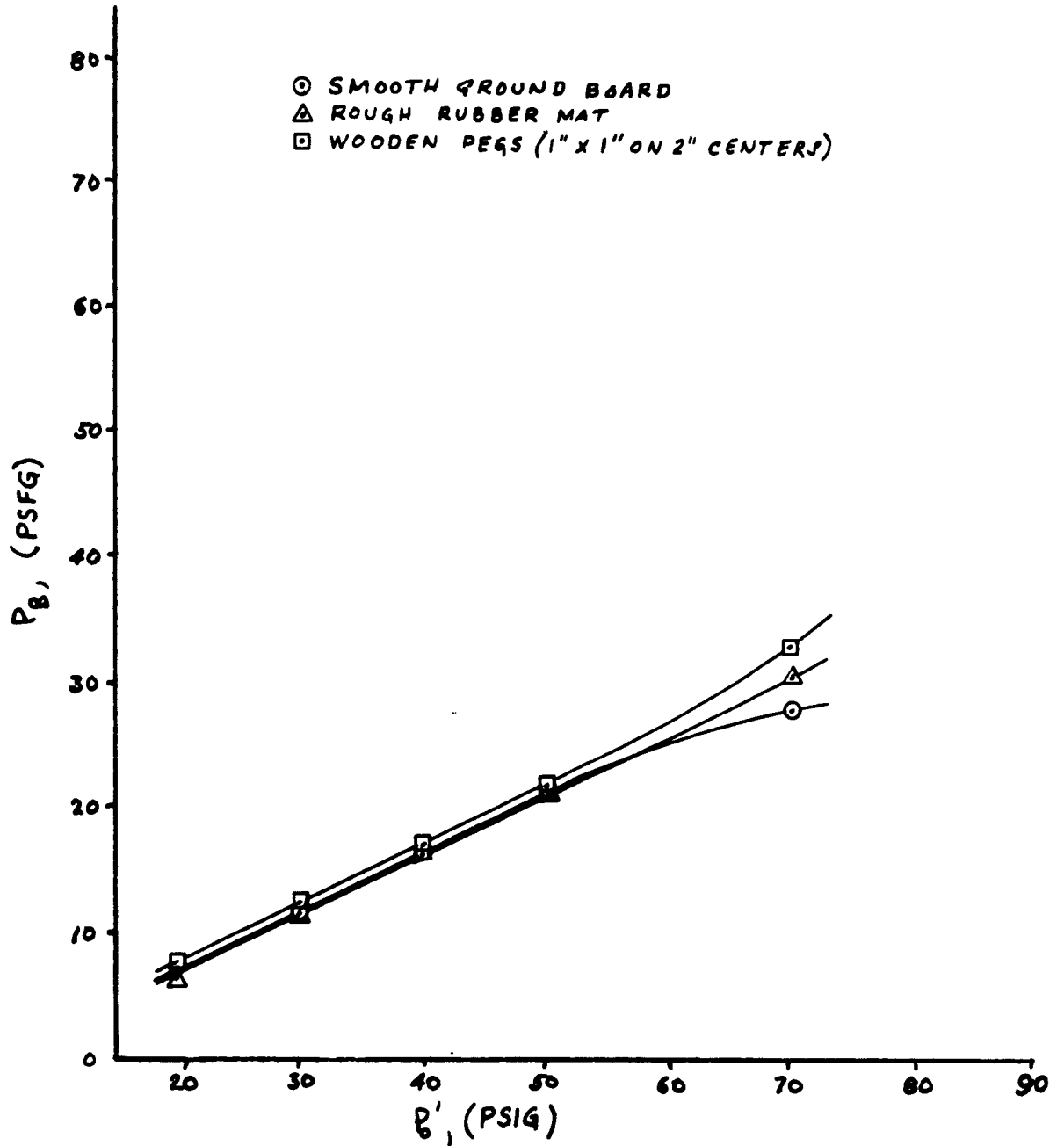


Figure 26. Effect of Surface Roughness for 2-D Tests

10 percent of the gross weight were performed while the vehicle was towed up to speeds of 10 miles per hour. These tests gave an indication of the dust characteristics of the recirculating curtain. Loose sand was encountered and was blown up and around the front of the vehicle; however, the quantity of sand which escaped the curtain was appreciably less than for a comparable annular vehicle.

Spray patterns over water were observed both with the vehicle floating on the water surface and with the base suspended at approximately a 1-foot height. The amount of water spray escaping from the curtain was negligible, although considerable spray activity was observed beneath the base.

Movie coverage of the dust and water spray experienced was obtained and forms a part of this report. The film is available on loan from the U. S. Army Transportation Research Command.

STABILITY

Because it was not possible to obtain the design height, only a small amount of testing was done in the area of stability and control. These tests on stability and control were to have been included in a tethered flight program and a free flight program.

The wind tunnel tests on the small scale model (Reference 2), previously obtained two-dimensional experimental data (Reference 1), and the data obtained from the MCTV tests will be referred to in order to evaluate the expected range of stability and control of the present vehicle. The problem areas encountered are pointed out and the presently available means for alleviating or correcting these is presented.

Heave Stability

The plots of base pressure versus height, as shown in Figures 27 through 29, demonstrate inherent heave stability over the expected operating range of the vehicle, i.e., height over 6 inches. Even the presence of a peak in this curve does not necessarily constitute a limiting point to the stability range. As an example of this, assume that the starting height is at point A of Figure 30. This height is any height greater than the height at which the peak occurs. (Note that the lift versus height curve will have approximately the same shape as the P_B versus height curve since the total lift is mainly dependent on base pressure as was shown in the wind tunnel tests of Reference 2).

When the machine is disturbed in heave such that it translates from h_A to h_B , the increased lift generated at h_B is stabilizing and will cause the vehicle to move back to h_A . In the same manner, if the machine translates from h_A to h_C , the lift generated at h_C will also be greater than that at h_A and will again be stabilizing. The limiting height in this case for positive stability in heave occurs at h_D since the lift at all heights between h_D and h_A is greater than

MODEL 3 RECIRCULATING EJECTOR $\theta_1 30^\circ, \theta_2 30^\circ$

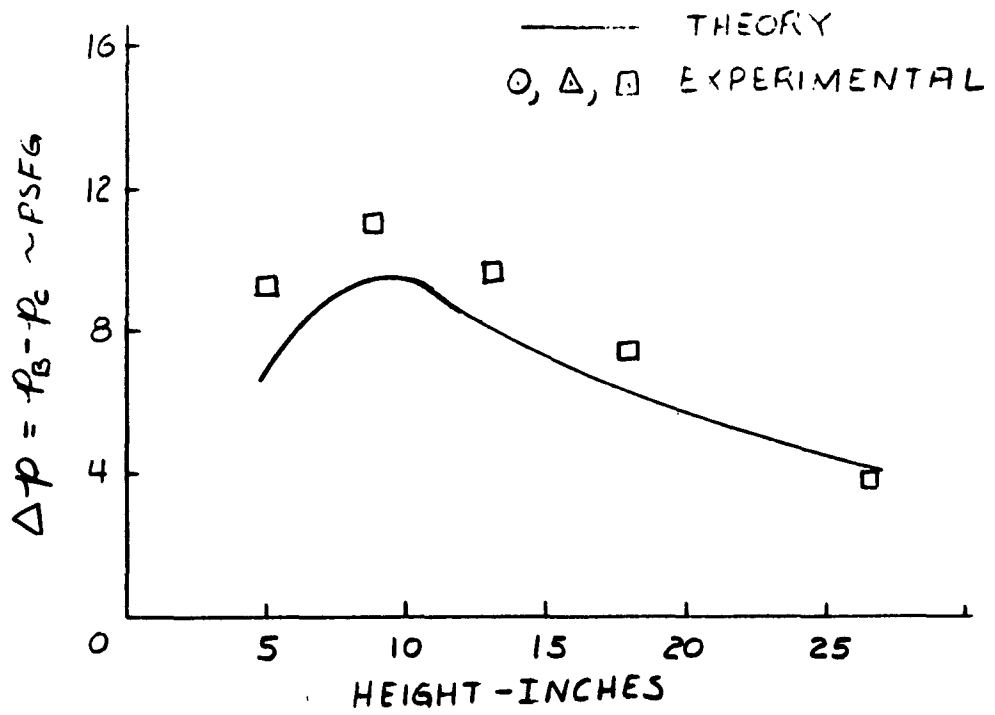
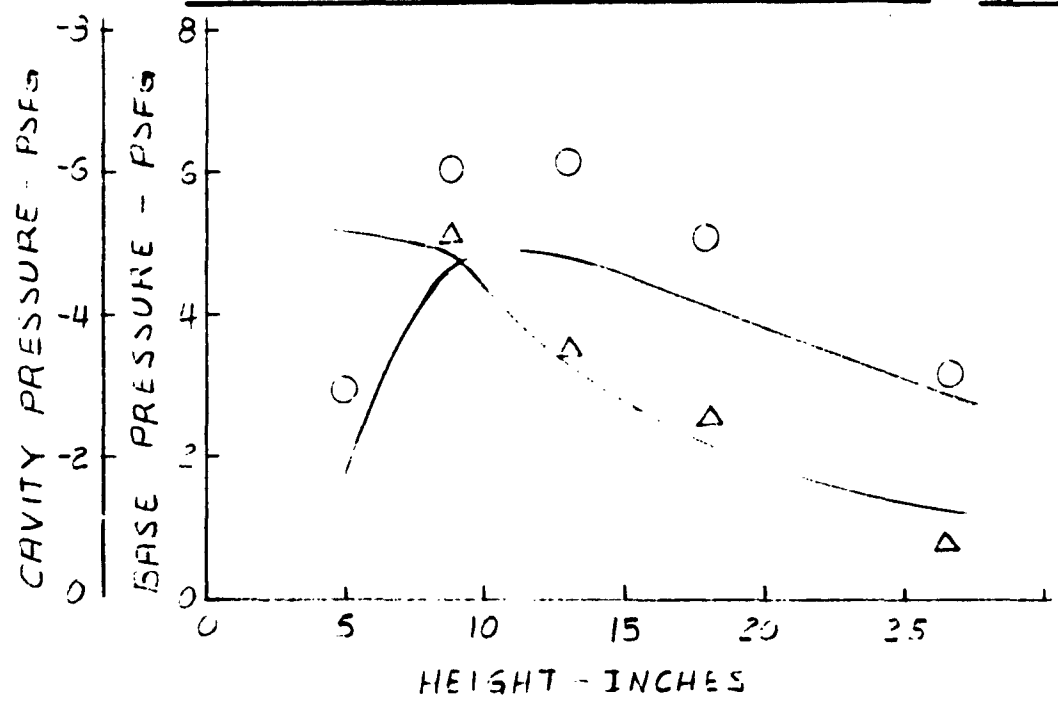


Figure 27. Comparison of Theory and Experiment for Base Pressure and Cavity Pressure

MODEL 3 RECIRCULATING EJECTOR $\theta_1 = 30^\circ, \theta_2 = 45^\circ$

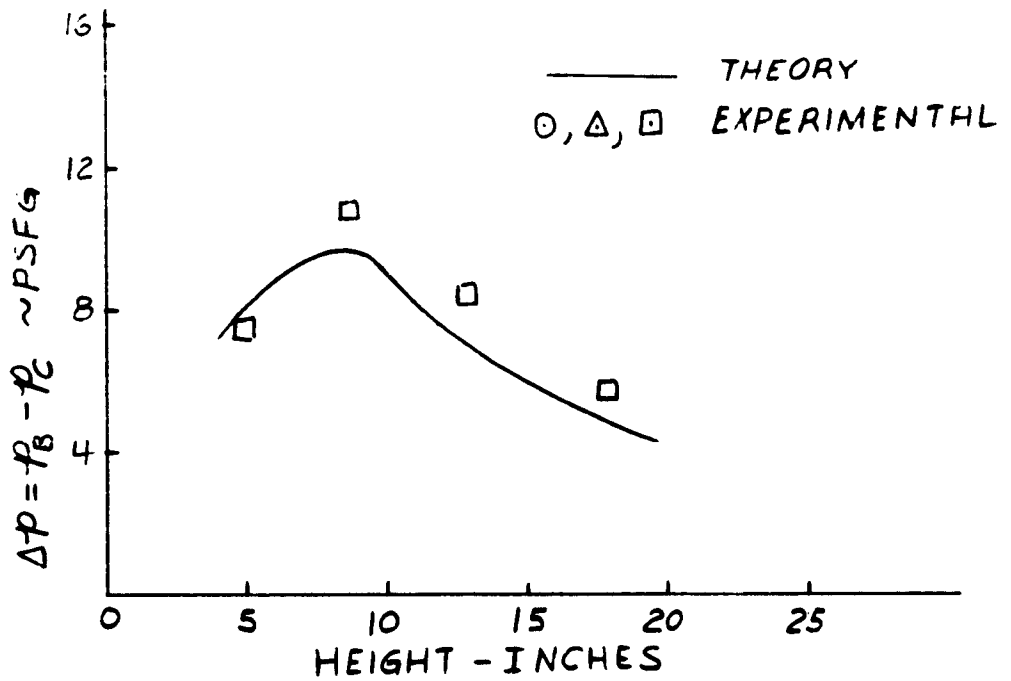
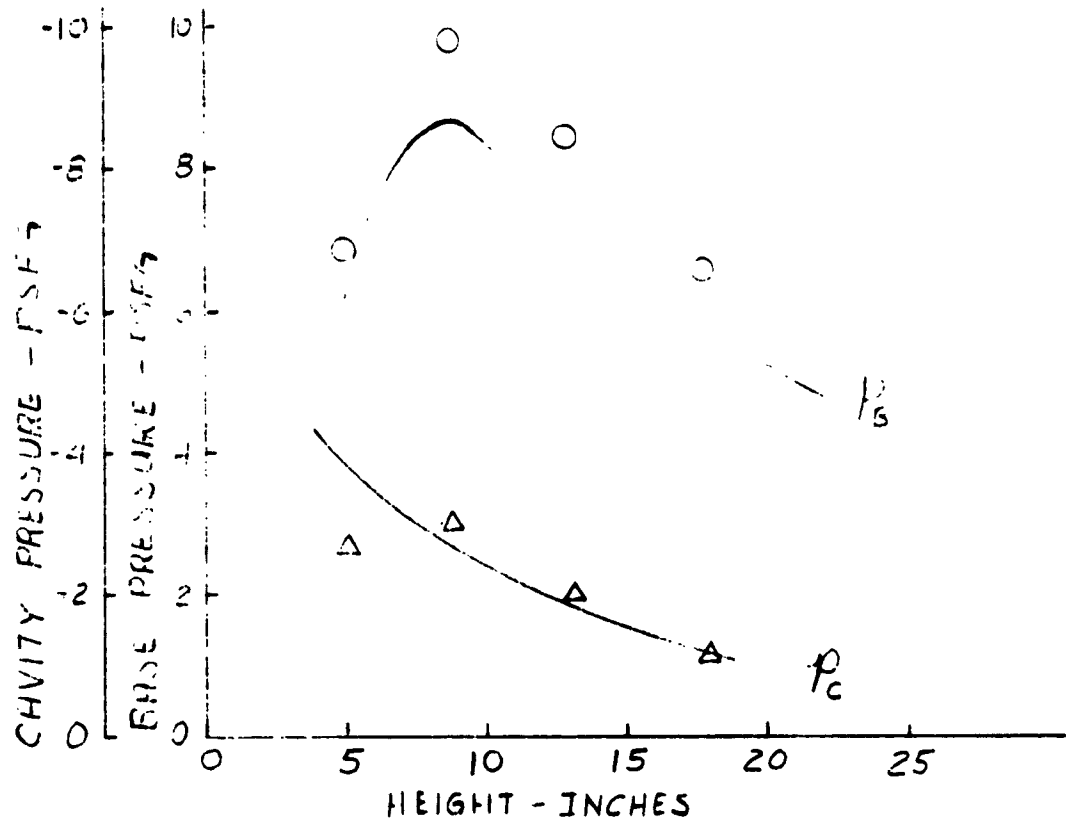


Figure 28. Comparison of Theory and Experiment for Base Pressure and Cavity Pressure

MODEL 3 RECIRCULATING EJECTOR $\theta_1 = 30^\circ, \theta_2 = 30^\circ$

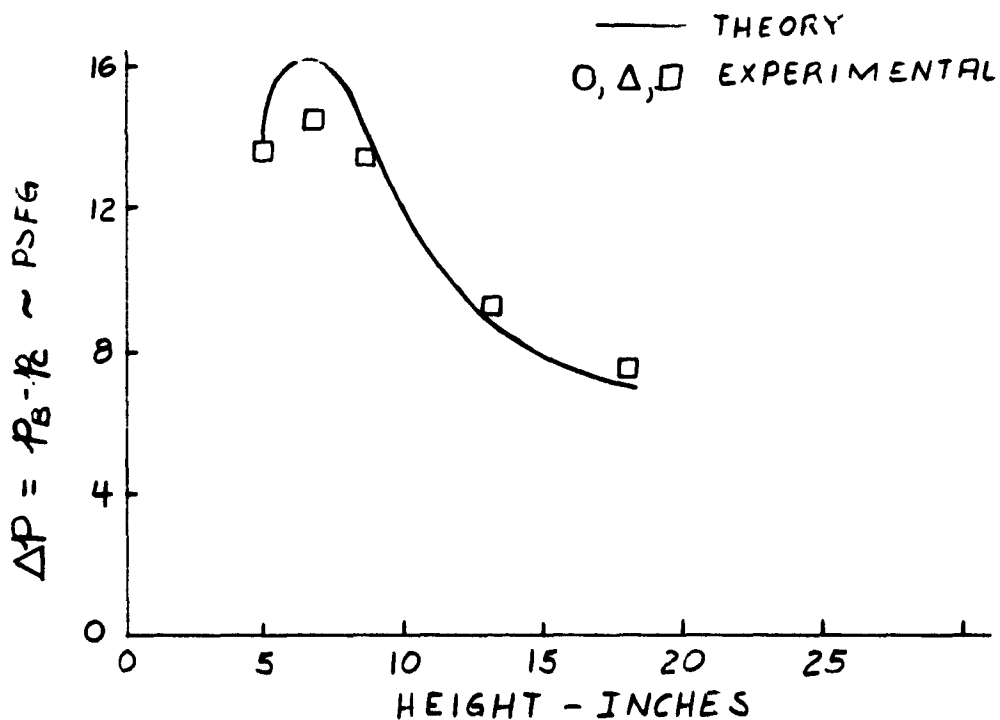
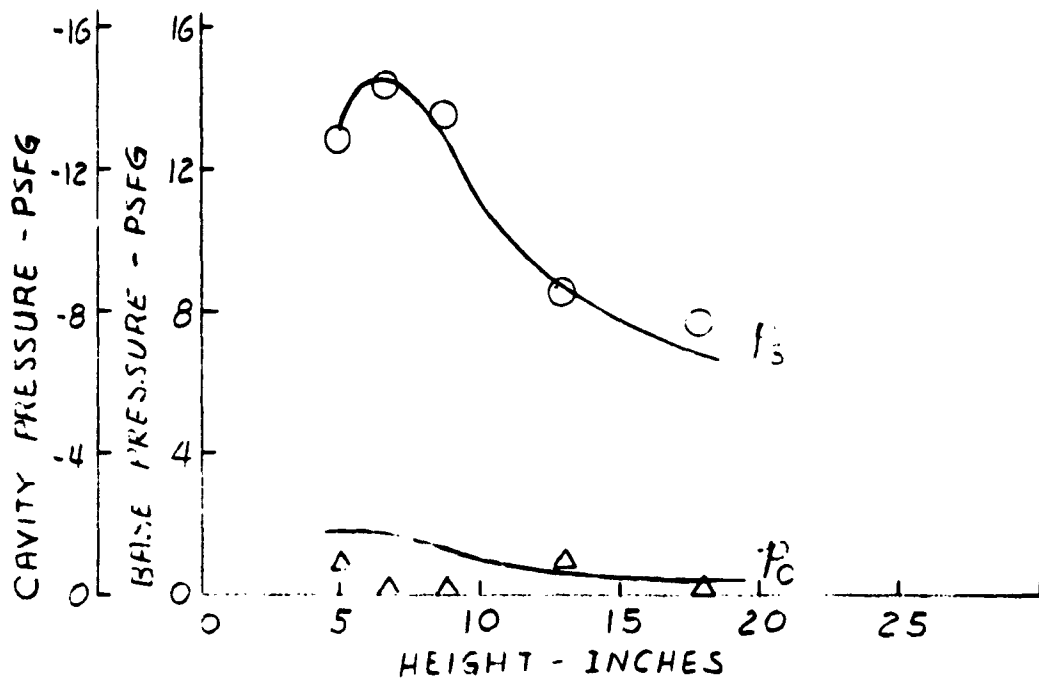


Figure 29. Comparison of Theory and Experiment for Base Pressure and Cavity Pressure

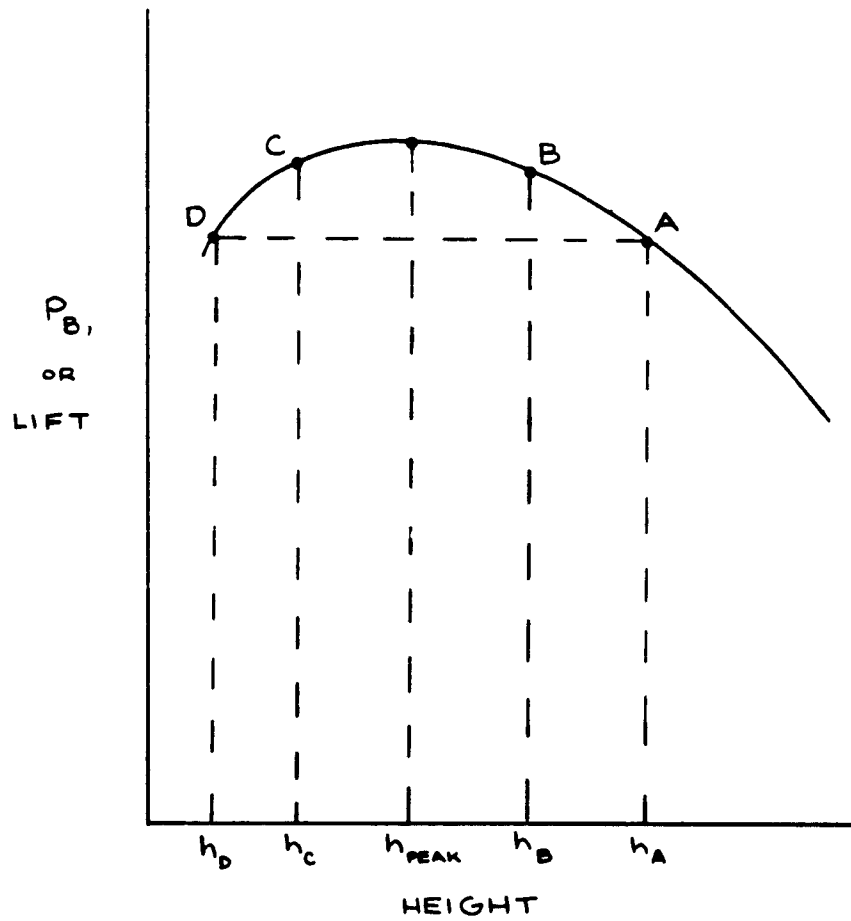


Figure 30. Lift versus Height

that at h_A . The machine is then stable in heave over the range $h \geq h_D$ when the initial height is h_A . All heights above h_A are stabilizing also, since the lift decreases with increasing heights.

This example points out the importance of operating above the peak point in a hovering condition or, conversely, it emphasizes the need for keeping the peak point at as low a height as possible. Fortunately, the means for increasing the efficiency of the ejector, i.e., low pressure primary air and the resultant low mass augmentation, results in either shifting the peak to the left or the elimination of the peak completely. This can be seen from the equations for cavity and base pressures from Reference 1.

$$P_C = -\frac{j}{h} \left[1 - \frac{2}{m/m'} - \cos \theta_2 \right]$$

$$P_B = \Delta p + p_C = \frac{j}{2t} \left[1 - e^{-2 \left(\frac{t}{h} \right) (1 + \cos \theta_1)} \right] - \frac{j}{h} \left[1 - \frac{2}{m/m'} - \cos \theta_2 \right]$$

Since the base pressure is dependent on the pressure jump across the recirculated stream, Δp , and the cavity pressure, p_C , the peak can be made to occur at lower heights by forcing the cavity pressure to have a smaller influence on the base pressure. Two methods are available to do this from inspection of the equation for p_C . They are:

1. Geometric design so that θ_2 is made as small as possible.
2. Aerodynamic design so that m/m' is decreased.

Both of these methods result in a more positive value of p_C for a given value of j/h , and in the case where $\frac{2}{m/m'} > (1 - \cos \theta_2)$, the cavity pressure can be made positive.

An example of the geometric method is presented in Figures 27 through 29. In these tests the discharge angle, θ_2 , was changed from 60° to 45° and then to 30° . The peak points occurred at 0.9, 0.7, and 0.5 feet respectively on these tests, showing the effect of this geometric change. A further decrease could then have been obtained by decreasing the mass augmentation from the level obtained in the ejector, i.e., $20 \leq m/m' \leq 30$. Ideally, if the mass augmentation were made lower than 14.9 for the $\theta_2 = 30^\circ$ ejector, the cavity pressure could be made positive and the peak could be virtually eliminated, since the base pressure would not then be degraded by the presence of a negative cavity pressure.

Intuitively, the problem of flow attachment would be relieved when the lower mass augmentation ratio is used. In the extreme case where the mass augmentation is 1 (that is, the annular jet), no flow is recirculated and thus the flow attachment problem is not encountered. In the case of high mass augmentation ratios, where the cavity pressure is negative even with detached flow, the jet has a tendency to attach

with the flat discharge angles required in recirculation. Thus, as the system moves from the high mass augmentation regime to the low mass augmentation regime, the problem of attachment should be less severe, especially when the mass augmentation is low enough to create positive cavity pressures.

Pitch Stability

In this section, use is made of an analytical method for computing the cavity pressure's contribution to pitch or roll stability (Reference 1), the wind tunnel report on the small scale model (Reference 2), and the data obtained on the MCTV.

The following is a brief résumé of the analytical program on the cavity pressure's contribution to stability. The equation for p_c is:

$$p_c = -\frac{j}{h} \left[1 - \frac{2}{m/m'} - \cos \theta_2 \right]. \quad (1)$$

In the case of a pitched machine, assuming that j and m/m' remain fixed, the equation becomes:

$$p_c = -\frac{j}{h + \frac{\omega}{2} \sin \alpha} \left[1 - \frac{2}{m/m'} - \cos (\theta_2 + \alpha) \right]. \quad (2)$$

The expression for the change in height and discharge angle can be obtained from Figure 31.

The moment due to p_c is:

$$\begin{aligned} \text{Moment} &= p_c \times S_c \times \bar{\ell} \\ &= -\frac{j}{h + \frac{\omega}{2} \sin \alpha} \left[1 - \frac{2}{m/m'} - \cos (\theta_2 + \alpha) \right] S_c \bar{\ell} \quad (3) \end{aligned}$$

where S_c is the projected horizontal area over which p_c acts and $\bar{\ell}$ is the moment arm of the air load due to cavity pressure.

The effect of p_c on the pitching moment is obtained by differentiating equation (3) with respect to :

$$\begin{aligned} \frac{\partial \text{Moment}}{\partial \alpha} &= \frac{\partial}{\partial \alpha} \left\{ -\frac{j}{h + \frac{\omega}{2} \sin \alpha} \left[1 - \frac{2}{m/m'} - \cos (\theta_2 + \alpha) \right] S_c \bar{\ell} \right\} \\ &= \frac{\partial j}{\omega} S_c \bar{\ell} \left\{ \frac{1}{\left(\frac{2h}{\omega} + \sin \alpha \right)} \left[\sin (\theta_2 + \alpha) \right] + \left[1 - \frac{2}{m/m'} - \cos (\theta_2 + \alpha) \right] \right. \\ &\quad \left. \left[\frac{-\cos \alpha}{\left(\frac{2h}{\omega} + \sin \alpha \right)^2} \right] \right\} \end{aligned}$$

$$= - \frac{2j}{\omega} s_c \bar{\ell} \left[\frac{\left(\frac{2h}{\omega} + \sin \alpha\right) \sin (\theta_2 + \alpha) - 1 - \left[\frac{2}{m/m'} - \cos (\theta_2 + \alpha)\right] \cos \alpha}{\left(\frac{2h}{\omega} + \sin \alpha\right)^2} \right] \cos \alpha \quad (4)$$

For the case of zero pitch, i.e., $\alpha = 0$, the derivative becomes:

$$\frac{\partial \text{Moment}}{\partial \alpha} = - \frac{2j}{\omega} s_c \bar{\ell} \left[\frac{\frac{2h}{\omega} \sin \theta_2 - \left(1 - \frac{2}{m/m'} - \cos \theta_2\right)}{\left(\frac{2h}{\omega}\right)^2} \right] \quad (5)$$

The cavity pressure is therefore stabilizing when this derivative is negative or when the bracketed term is positive. Assuming that $\left(\frac{2h}{\omega}\right)^2 = 0$, the criteria for p_c to be stabilizing is then:

$$\left[\frac{2h}{\omega} \sin \theta_2 - \left(1 - \frac{2}{m/m'} - \cos \theta_2\right) \right] > 0. \quad (6)$$

The equation also defines a height at which the cavity pressure has a neutral effect on pitch stability. This height can be obtained by setting the left side of equation (6) equal to zero.

$$\frac{2h}{\omega} \sin \theta_2 - \left(1 - \frac{2}{m/m'} - \cos \theta_2\right) = 0$$

The nondimensional height for neutral stability due to cavity pressure is:

$$\frac{2h}{\omega} = \frac{1 - \frac{2}{m/m'} - \cos \theta_2}{\sin \theta_2} \quad ..$$

All heights above this neutral height will be stabilizing with regard to cavity pressures.

A comparison is made between this analytical method for predicting the neutral stability height and the height at which neutral stability in pitch was obtained on the wind tunnel model of Reference 2. The runs using $p'_0 = 67.5$ with $V_\infty = 0$ are used for comparison. Since the mass augmentation varied with height, it was necessary to plot the measured mass augmentation versus height and then to cross-plot the predicted neutral height versus mass augmentation. The height corresponding to neutral stability occurs at the intersection of the two curves as shown in Figure 32. The actual height for neutral stability is shown in Figure 33. The unstable region extends to $h = 2.35$ inches while the predicted value is $h = 2.25$ inches, showing a good correspondence between the predicted value and the experimental one,

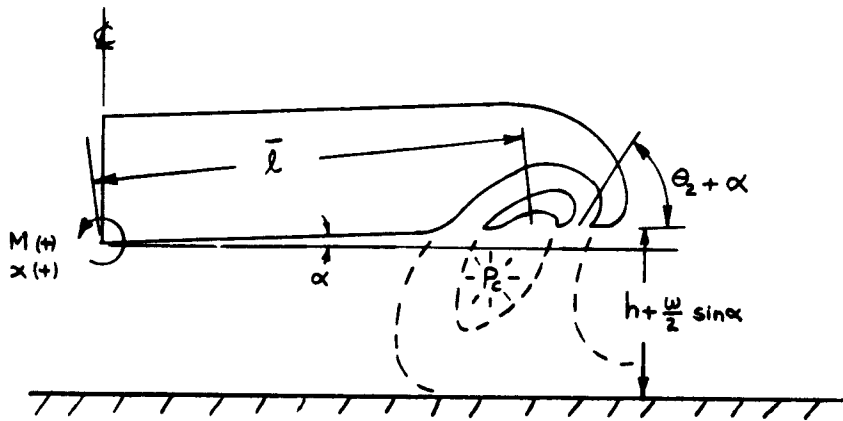
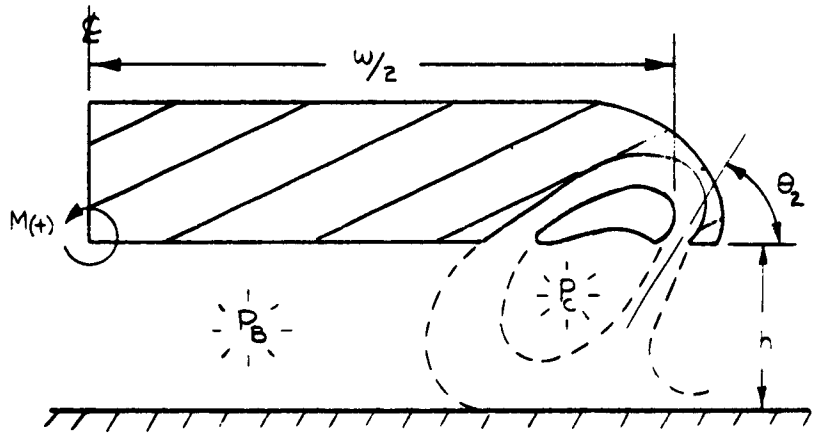


Figure 31. Schematic, Pitch Stability

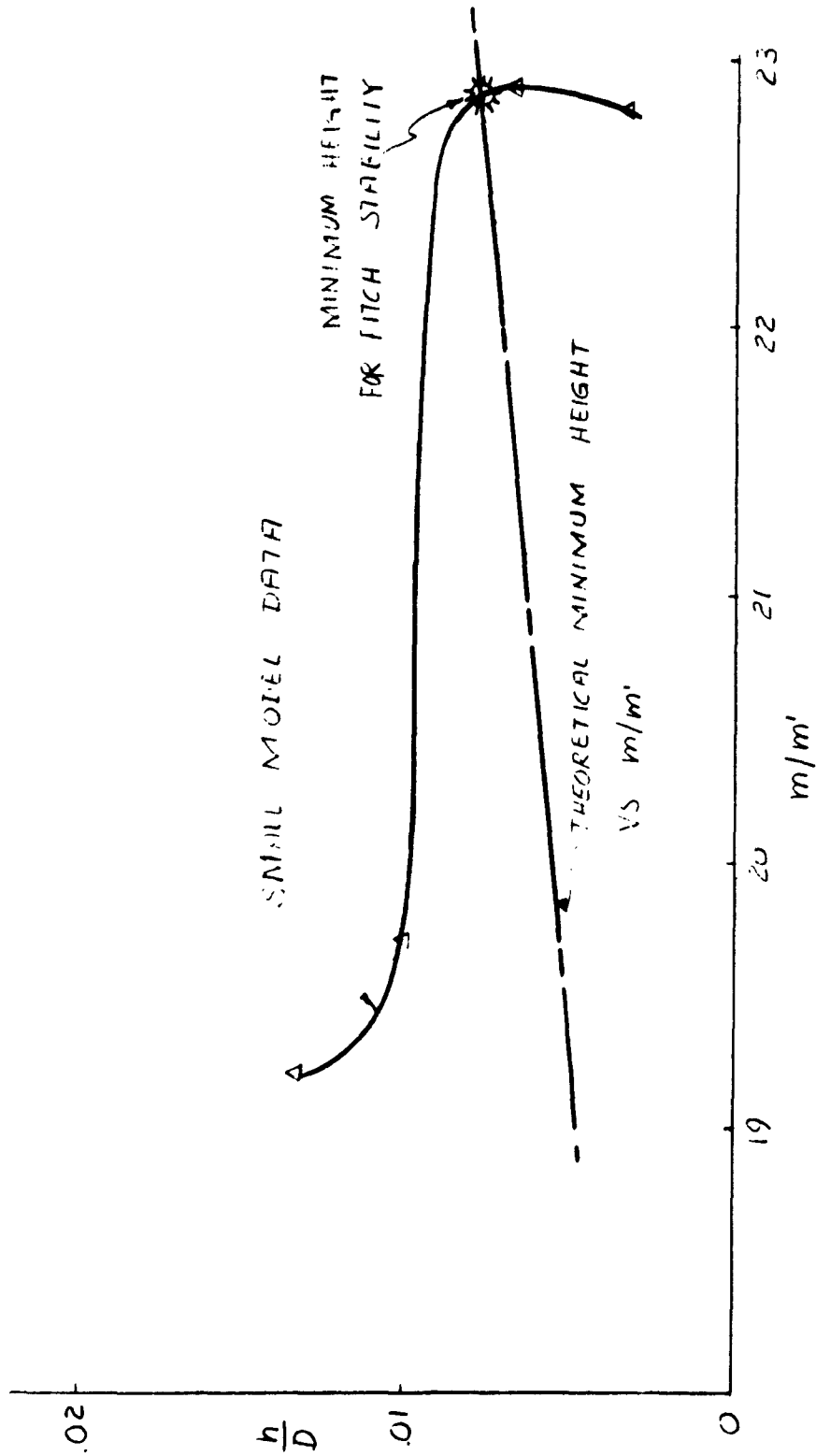


Figure 32. Theoretical and Experimental Curve for Mass Augmentation and Minimum Height for Positive Stability in Pitch, Wind Tunnel Model

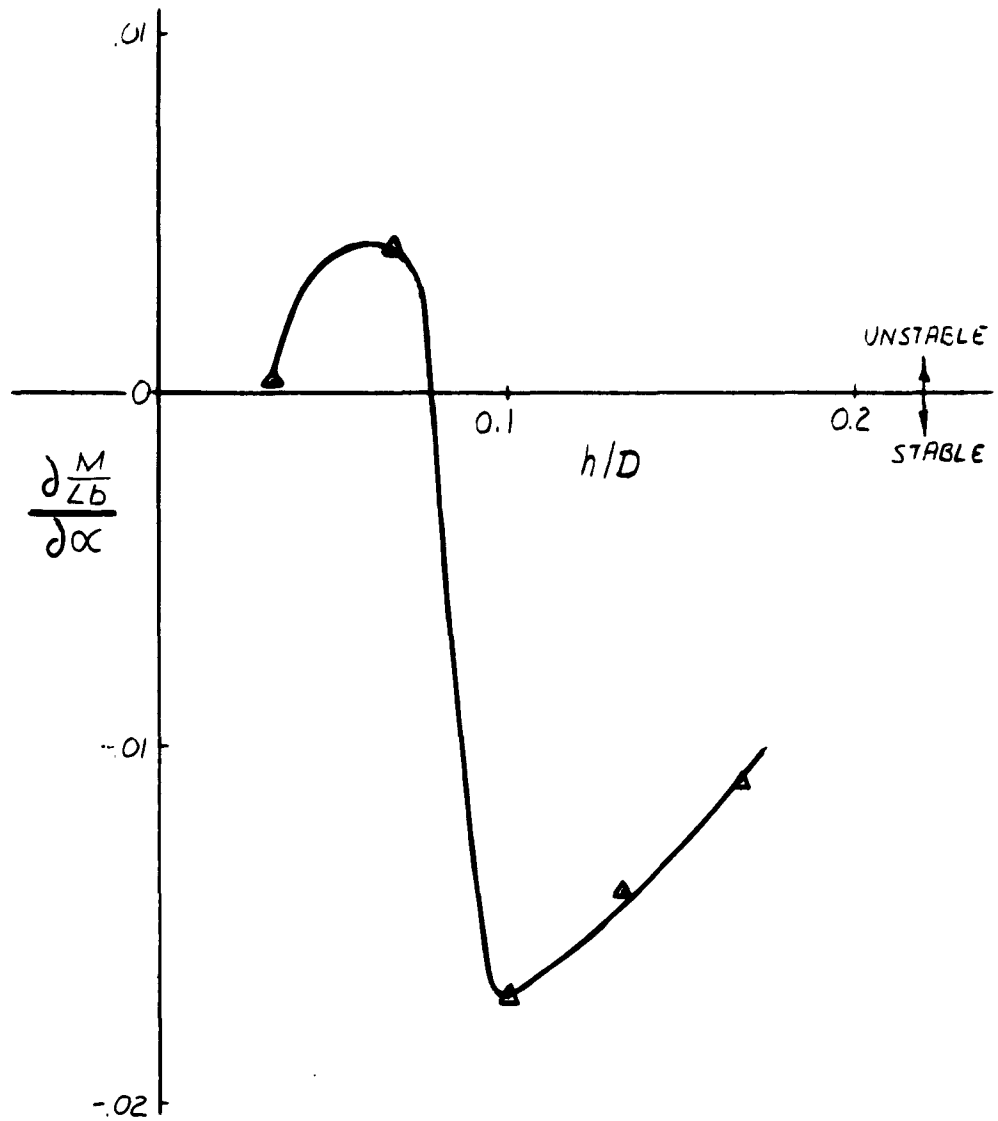


Figure 33. Minimum Height for Positive Stability of the Small Scale Wind Tunnel Model in Pitch

although this good agreement must be tempered somewhat by the fairings required through the wide variation in data in both applicable curves.

Applying the same analytical method to the MCTV, where the mass augmentation was measured to be approximately 30 at 10.5 inches, the height for neutral stability is 16.2 inches for $\theta_2 = 30^\circ$ as shown in Figure 34.

There are then means available to cause the cavity pressure to be stabilizing in pitch with the present geometry. They are:

1. Power the MCTV so that it can hover at a height greater than 16.2 inches.
2. Lower the mass augmentation so that the minimum height can be lowered accordingly. As an example, with $m/m' = 17.5$, the neutral height can be reduced to 4.8 inches; or with $m/m' < 15$, this method would indicate a stabilizing effect at all heights.

The variation in base pressure from the front to the rear of the base was measured at one height for several pitch angles and is shown in Figure 35. This variation in base pressure shows the base pressure to be stabilizing in pitch. The interrelationship between pitch stability and heave stability can be seen by the degradation of the average pressure in the pitch case compared to the zero pitch case.

In the pitch stability analysis, then, as well as in the heave stability analysis, the use of low-pressure air with its resultant low mass augmentation will cause the machine to be stable over a wider range of heights. One additional problem is encountered at the lower mass augmentations. This is the determination of the effects of cross flow under the base of the machine. In the lower mass augmentation regime, more air is expelled from the system per unit time and the variation in lifting pressure distribution under the machine needs to be investigated both experimentally and analytically.

No additional analysis is made here of stability in roll due to the similarity to the stability in pitch analysis.

CONTROL EFFECTIVENESS

Only a small amount of experimental data is available pertaining to control forces available on the MCTV. In one test, visual observation was used to determine an approximate pitching moment obtained from the ejectors. Another instrumented test was run to determine the effect of base pressure distribution on control moments. These trends were evaluated by measuring the base pressure at six points on the base.

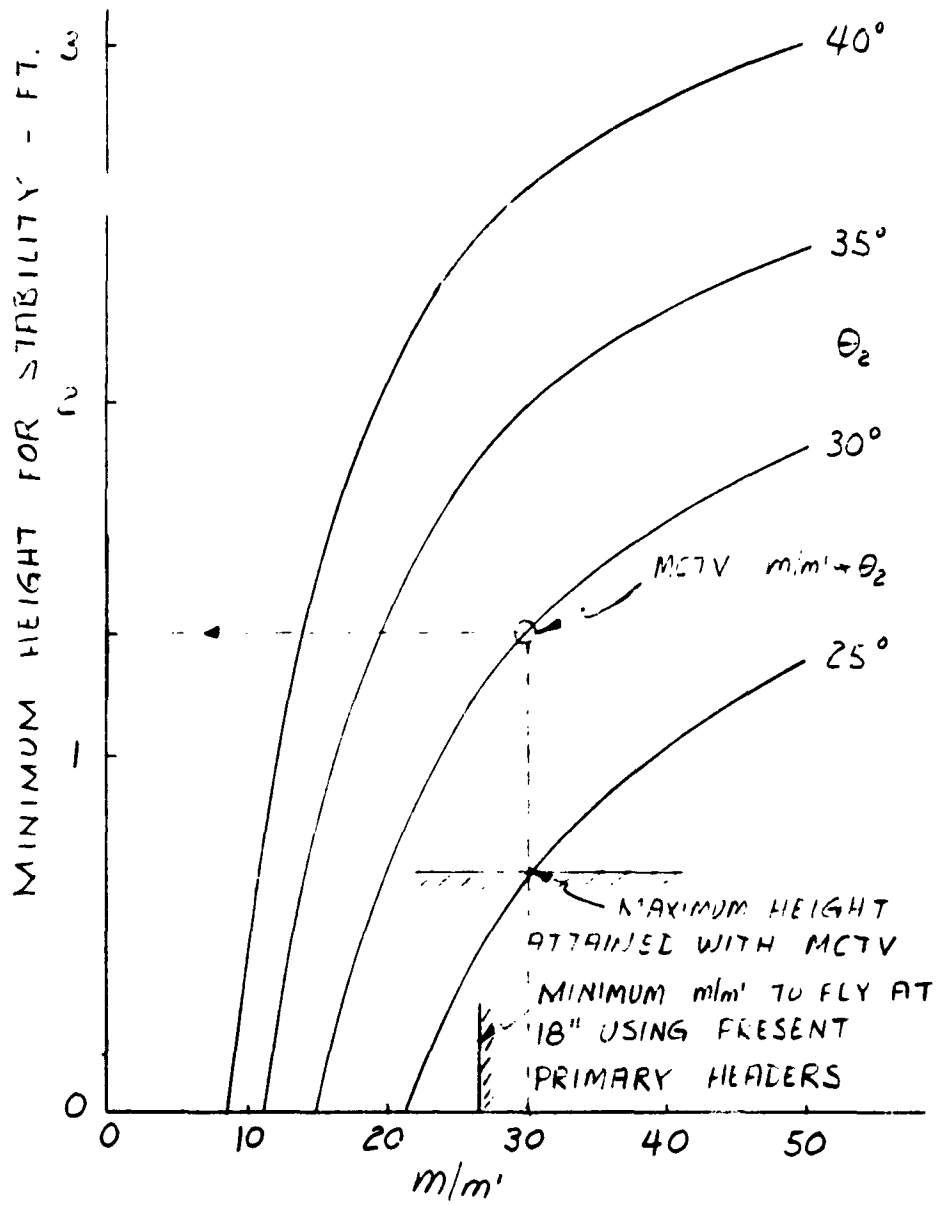


Figure 34. Minimum Height for Cavity Pressure Stability

CENTER HEIGHT CONSTANT AT 10 INCHES
 $P_0' = 35 \text{ PSIG}$

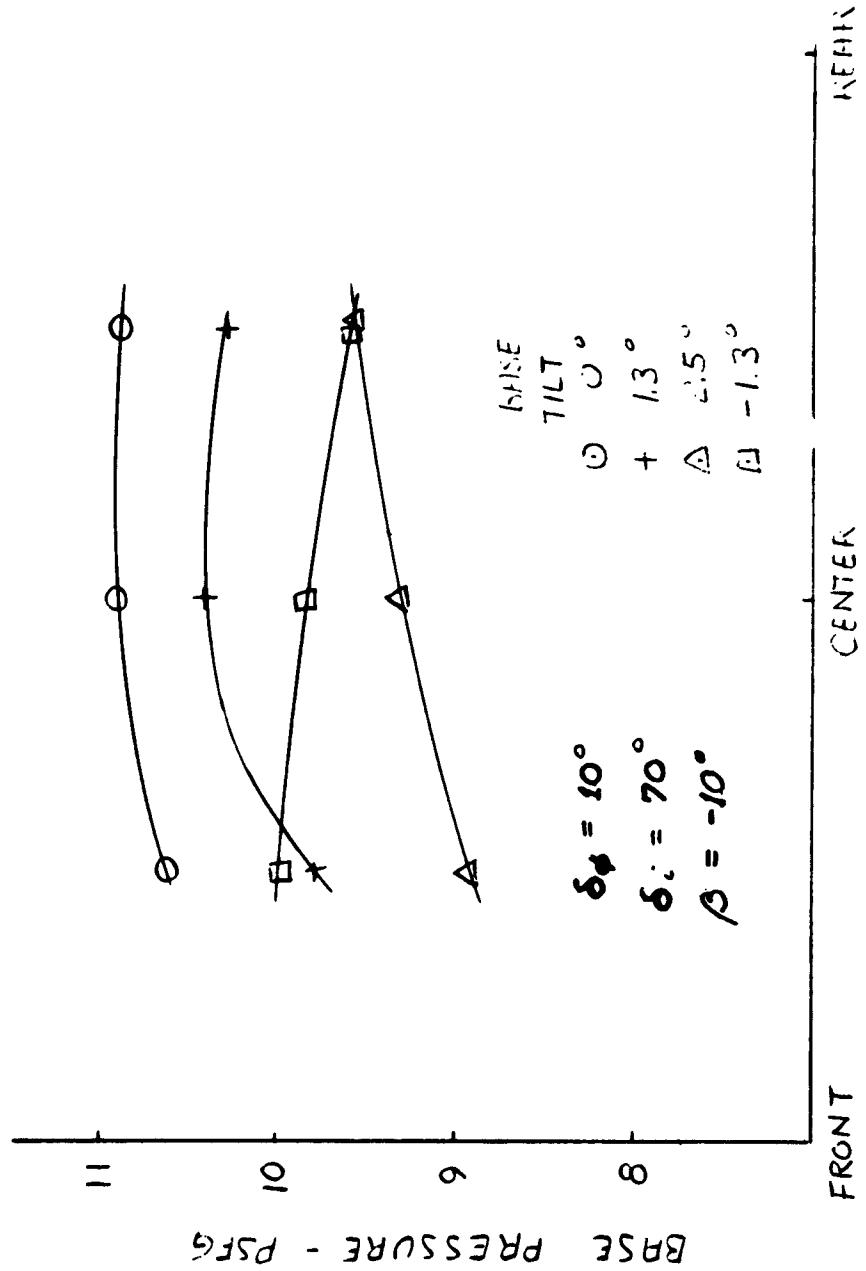


Figure 35. Effect of Base Tilt on Base Pressure with Controls Locked in Neutral Position

In the first test, when the full load of water and fuel was on board, there was an unbalance of approximately 566 foot-pounds, as shown in Figure 36.

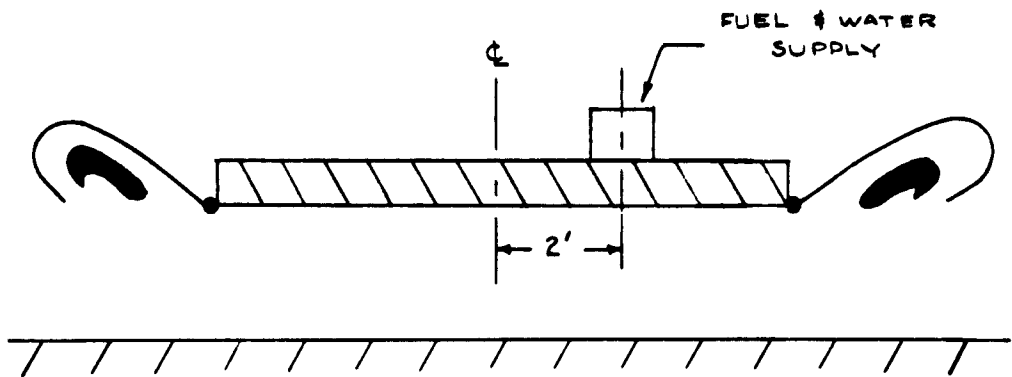
It was found that the controls were not able to counteract this unbalance; but when the fuel and water load was down to one-half the original load, the controls became effective, indicating that they could create a pitching moment of approximately 283 foot-pounds.

The momentum force, j , was measured to be 8 pounds per foot, while j' was calculated to be 3.76 pounds per foot. With the ejector configuration used, this combination of j and j' should create a pitching moment of 267 foot-pounds, showing good agreement with the observed results.

During the course of the testing, six pressure taps were installed on the base of the machine as shown in Figure 5 to determine base pressure contribution to the control moments produced by the ejectors. This testing was carried out to see if the trends indicated by the base pressure distribution aided the control moments or acted in opposition to them. It must be stressed that, due to the small number of taps used, only the general trends were obtained.

The rolling moments and pitching moments were calculated by a matrix technique assuming that the pressure variation was linear between points and stations. The platform was assumed to be completely rectangular by neglecting the chopped corners.

Base pressure contribution to control moments is shown in Table 1.



Unbalanced Weights

Water	18 gallons	151 lb
Fuel	22 gallons	<u>132 lb</u>
		= 283 lb

Moment = 283 pounds x 2 ft = 566 ft-lb

Figure 36. Control Effectiveness Test

Table 1
Base Pressure Contribution to Control Moments

ξ	-10		-10		-10		-10	
h	6		6		10		10	
P _o '	32		32		32		32	
$\delta\phi$	10		10		10		10	
δi	40		70		40		70	
Control Code	L ft-lb	M ft-lb	L ft-lb	M ft-lb	L ft-lb	M ft-lb	L ft-lb	M ft-lb
1	0	4	-21	-36	-31	17	-62	40
2	-	24	-	3	-	28	-	-57
3	-	9	-	62	-	+ 4	-	-90
4	-	-14	-	-48	-	61	-	-299
5	0	-	42	-	-21	-	-63	-
6	63	-	147	-	+21	-	-42	-
7	-84	-	42	-	0	-	-126	-

Control Position Code

- 1 = Neutral
- 2 = 5° Pitch Up
- 3 = 10° Pitch Up
- 4 = 10° Pitch Down
- 5 = 10° Right Roll
- 6 = 20° Right Roll
- 7 = 20° Left Roll

The general trends of these tests indicate that in the roll condition the base pressure distribution due to ejector tilt results in a moment that aids that produced by the ejectors. The trend in the pitch case is more erratic than in the roll case, but except for one case the moments obtained are quite small. In a more exact study of this effect, many more base pressure taps would be required, especially in the region of rapidly changing base pressure such as occurs near the inlet of the ejectors.

Recommended Modifications

It is apparent from results of flight testing of the vehicle that some basic modifications to the ejectors are necessary to obtain satisfactory performance. The ejector design incorporated in the vehicle was dictated by the air flow and pressure from the available engines. Model 5 ejector represented the best attainable performance utilizing this air source.

More recent experimental data indicate that significantly improved performance is attainable using a high mass flow, low-pressure air supply. These data are shown in Figure 37 where base pressure is plotted against ejector area ratio. These data have been corrected for the 2-D and 3-D performance loss observed on the vehicle. Test data have been obtained at area ratios as low as 75. There is a trend toward improved performance at the low area ratios, which is apparently due to better mixing between two streams of more nearly equal velocities. Although further 2-D tests at area ratios below 73 are required for verification, it appears that 375 HP at 10 psig would lift the vehicle at 18 inches while 375 HP from the AiResearch engines at 34 psi is totally inadequate. These figures are conservative since they include a 25-percent loss factor correcting 2-D, 3-D performance.

Experimental investigation of the source of the loss in performance between 2-D and 3-D is required. Small scale model tests indicated that 2-D performance could be obtained in a 3-D configuration. Therefore, it appears that the loss in base pressure incurred on the vehicle is peculiar to the vehicle geometry. Quite likely, the loss is largely due to corner leakage. During testing of the vehicle, it was noted that an abnormal proportion of air leakage occurred in the area of the corners.

Finally, a high mass flow, low-pressure air source is required as the lifting power plant. Although final selection of the optimum mass flow and pressure combination must await further 2-D tests, a power plant delivering 12 pounds per second at 10 psig (400 air horsepower) should be adequate.

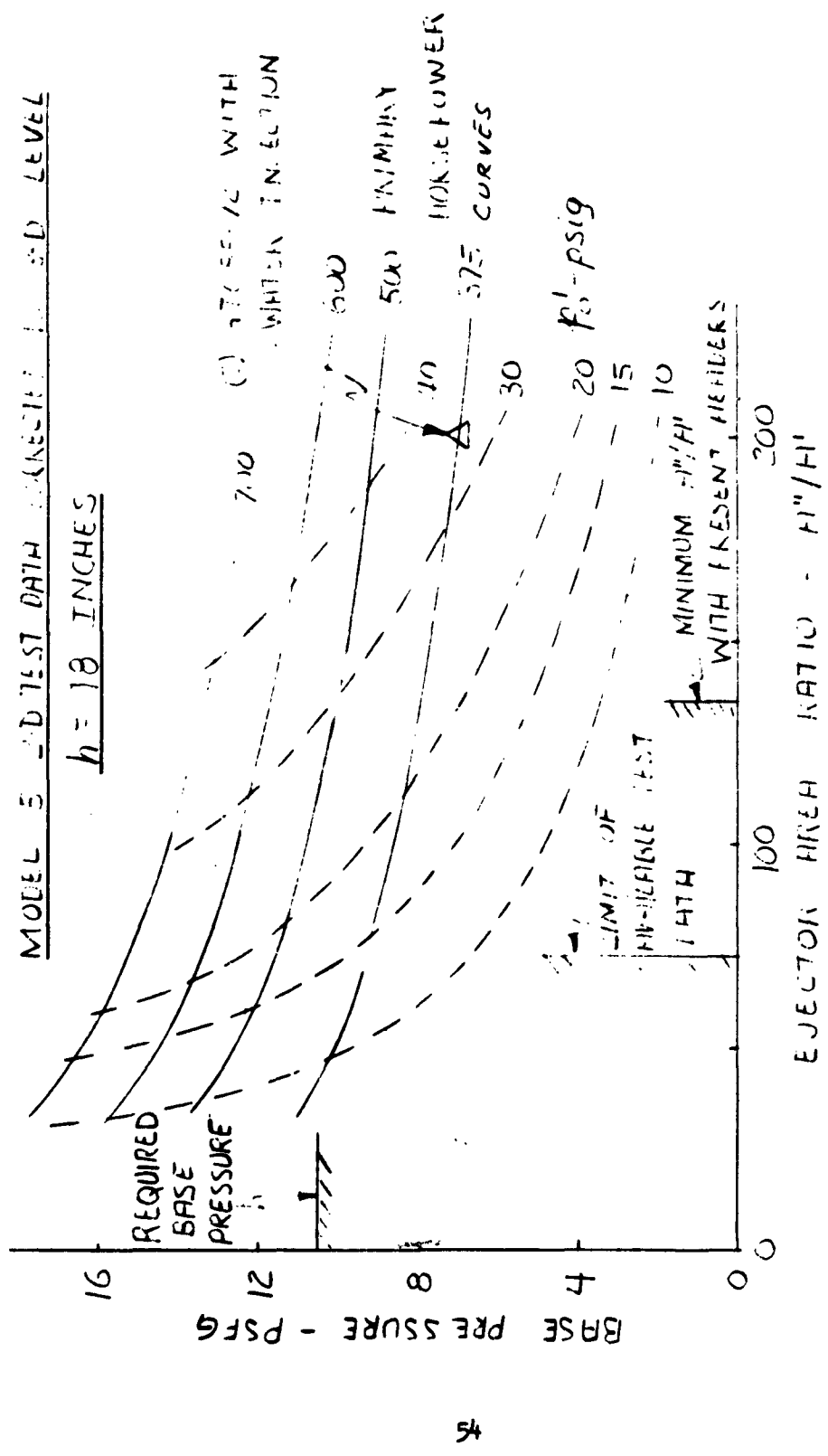


Figure 37. Effect of Ejector Area Ratio and Primary Pressure on Base Pressure

REFERENCES

- 1 Ortell, A., et.al., "Recirculating Principle for Ground Effect Machine, Two-Dimensional Tests", TCREC Technical Report 62-66, June 1962
- 2 Vinson, P., et.al., "Recirculation Principle for Ground Effect Machine, Three-Dimensional Wind Tunnel Tests", TCREC Technical Report 62-74, July 1962
- 3 Butsko, J., et.al., "Recirculation Principle for Ground Effect Machine, Man-Carrying Test Vehicle and Component Testing", TCREC Technical Report 62-99 (not released)

DISTRIBUTION

USAWC	1
USATMC(FTZAT),ATO	1
USAPRDC	1
DCSLOG	1
Rsch Anal Corp	1
ARO, Durham	2
OCRD, DA	2
NATC	1
ARO, OCRD	1
DCSOPS	1
USAERDL	2
USATAC, Center Line	3
OrdBd	1
USATCDA	1
USATMC	19
USATSCH	4
USATRECOM	62
TCLO, USAABELCTBD	1
USATRECOM LO, USARDG (EUR)	3
CNO	1
ONR	3
BUWEPS, DN	2
ACRD(OW), DN	1
USNSRDF	1
USNPGSCH	1
BUSHP, DN	1
USNOTS	1
Dev Tay Mod Bas	1
MCLFDC	1
MCEC	1
USASGCA	1
Canadian LO, USATSCH	3
BRAS, DAQMG(Mov & Tn)	4
USASG, UK	1
Langley Rsch Cen, NASA	2
Ames Rsch Cen, NASA	2
Lewis Rsch Cen, NASA	1
Sci & Tech Info Fac	1
USGPO	1
ASTIA	10
USAMRDC	1
HumRRO	2
ODDR&E, Comm. on Aeronautics	1
US Maritime Adm	1
Hum Engr Lab	1
USAMOCOM	3
USSTRICOM	1
Martin Co.	10

1. Recirculation Principle for Ground Effect Machine
Contract DA-44-177-TC-710
2. Contract DA-44-177-TC-710

AD Accession No
Martin Company, Orlando, Florida
 RECIRCULATION PRINCIPLE FOR GROUND EFFECT MACHINE MAN-CARRYING TEST VEHICLE PRELIMINARY FLIGHT TEST VEHICLE -
 P. Vinson
 TREC Technical Report 62-100, Final Report, December 1962, 55 pp - illustrations (Contract DA-44-177-TC-710)
 Task 9R99-01-005-04, Unclassified
 Results of an experimental investigation of hovering performance and stability and control characteristics of ground effect machine. Feasibility of obtaining lift by utilizing recirculating ejector concept was proven.

1. Recirculation Principle for Ground Effect Machine
Contract DA-44-177-TC-710
2. Contract DA-44-177-TC-710

AD Accession No
Martin Company, Orlando, Florida
 RECIRCULATION PRINCIPLE FOR GROUND EFFECT MACHINE MAN-CARRYING TEST VEHICLE PRELIMINARY FLIGHT TEST VEHICLE -
 P. Vinson
 TREC Technical Report 62-100, Final Report, December 1962, 55 pp - illustrations (Contract DA-44-177-TC-710)
 Task 9R99-01-005-04, Unclassified
 Results of an experimental investigation of hovering performance and stability and control characteristics of ground effect machine. Feasibility of obtaining lift by utilizing recirculating ejector concept was proven.

1. Recirculation Principle for Ground Effect Machine
Contract DA-44-177-TC-710
2. Contract DA-44-177-TC-710

AD Accession No
Martin Company, Orlando, Florida
 RECIRCULATION PRINCIPLE FOR GROUND EFFECT MACHINE MAN-CARRYING TEST VEHICLE PRELIMINARY FLIGHT TEST VEHICLE -
 P. Vinson
 TREC Technical Report 62-100, Final Report, December 1962, 55 pp - illustrations (Contract DA-44-177-TC-710)
 Task 9R99-01-005-04, Unclassified
 Results of an experimental investigation of hovering performance and stability and control characteristics of ground effect machine. Feasibility of obtaining lift by utilizing recirculating ejector concept was proven.

1. Recirculation Principle for Ground Effect Machine
Contract DA-44-177-TC-710
2. Contract DA-44-177-TC-710

AD Accession No
Martin Company, Orlando, Florida
 RECIRCULATION PRINCIPLE FOR GROUND EFFECT MACHINE MAN-CARRYING TEST VEHICLE PRELIMINARY FLIGHT TEST VEHICLE -
 P. Vinson
 TREC Technical Report 62-100, Final Report, December 1962, 55 pp - illustrations (Contract DA-44-177-TC-710)
 Task 9R99-01-005-04, Unclassified
 Results of an experimental investigation of hovering performance and stability and control characteristics of ground effect machine. Feasibility of obtaining lift by utilizing recirculating ejector concept was proven.

AD _____
Accession No _____
Martin Company, Orlando, Florida
RECIRCULATION PRINCIPLE FOR GROUND EFFECT MACHINE MAN-CARRYING TEST VEHICLE PRELIMINARY FLIGHT TEST VEHICLE -
P. Vinson
TREC Technical Report 62-100, Final Report, December 1962, 55 pp - illu- s- tables (Contract DA-44-177-TC-710)
Task 9R99-01-005-04, Unclassified
Results of an experimental investigation of hovering performance and stability and control characteristics of ground effect machine. Feasibility of obtaining lift by utilizing recirculating ejector concept was proven.

1. Recirculation Principle for Ground Effect Machine
Contract DA-44-177-TC-710

AD _____
Accession No _____
Martin Company, Orlando, Florida
RECIRCULATION PRINCIPLE FOR GROUND EFFECT MACHINE MAN-CARRYING TEST VEHICLE PRELIMINARY FLIGHT TEST VEHICLE -
P. Vinson
TREC Technical Report 62-100, Final Report, December 1962, 55 pp - illu- s- tables (Contract DA-44-177-TC-710)
Task 9R99-01-005-04, Unclassified
Results of an experimental investigation of hovering performance and stability and control characteristics of ground effect machine. Feasibility of obtaining lift by utilizing recirculating ejector concept was proven.

1. Recirculation Principle for Ground Effect Machine
Contract DA-44-177-TC-710

AD _____
Accession No _____
Martin Company, Orlando, Florida
RECIRCULATION PRINCIPLE FOR GROUND EFFECT MACHINE MAN-CARRYING TEST VEHICLE PRELIMINARY FLIGHT TEST VEHICLE -
P. Vinson
TREC Technical Report 62-100, Final Report, December 1962, 55 pp - illu- s- tables (Contract DA-44-177-TC-710)
Task 9R99-01-005-04, Unclassified
Results of an experimental investigation of hovering performance and stability and control characteristics of ground effect machine. Feasibility of obtaining lift by utilizing recirculating ejector concept was proven.

1. Recirculation Principle for Ground Effect Machine
Contract DA-44-177-TC-710

AD _____
Accession No _____
Martin Company, Orlando, Florida
RECIRCULATION PRINCIPLE FOR GROUND EFFECT MACHINE MAN-CARRYING TEST VEHICLE PRELIMINARY FLIGHT TEST VEHICLE -
P. Vinson
TREC Technical Report 62-100, Final Report, December 1962, 55 pp - illu- s- tables (Contract DA-44-177-TC-710)
Task 9R99-01-005-04, Unclassified
Results of an experimental investigation of hovering performance and stability and control characteristics of ground effect machine. Feasibility of obtaining lift by utilizing recirculating ejector concept was proven.

1. Recirculation Principle for Ground Effect Machine
Contract DA-44-177-TC-710